Available online at www.sciencedirect.com
SCIENCE DIRECT
Lithos 89 (2006) 329–352
LITHOS
www.elsevier.com/locate/lithos

Marginal mafic intrusions as indicators of downslope draining of dense residual melts in anorthositic diapirs?

Jacqueline Vander Auwera [a,*], Dominique Weis [b], Jean Clair Duchesne [a]

[a] Department of Geology, Université de Liège, Belgium
[b] Department of Earth and Ocean Sciences, University of British Columbia, Vancouver, Canada

Received 29 October 2004; accepted 23 December 2005
Available online 20 February 2006

Abstract

Geochemical and isotopic investigation of three small mafic intrusions (Løyning: 1250 × 150 m, Hogstad: 2000 × 200 m, Koldal: 1250 × 500 m) in the marginal zones of the Egersund-Ogna (Løyning, Koldal) and Åna-Sira massif-type anorthosites (Hogstad) (Rogaland Anorthositic Province, south Norway: 930 Ma) provides new insights into the late evolution of anorthositic diapirs. These layered mafic intrusions are essentially of norite, gabbronorite as well as leuconorite and display conspicuous evidence of subsolidus recrystallization. In Løyning and Hogstad, the modal layering is parallel to the subvertical foliation in the enclosing anorthosite. The northern part of the Koldal intrusion cuts across the foliation of the anorthosite, whereas in its southern part the subvertical layering is parallel to the anorthosite's foliation. The regularity of the layered structures suggests that the layering was initially acquired horizontally and later tilted during the final movements of the diapirs.

The least differentiated compositions of plagioclase and orthopyroxene in the three intrusions (An_{59}–En_{68} in Løyning, An_{49}–En_{64} in Hogstad and An_{44}–En_{61} in Koldal) and the REE contents in apatite (Hogstad) indicate that their parent magmas were progressively more differentiated in the sequence Løyning–Hogstad–Koldal. Isotopic data (Løyning: $^{87}Sr/^{86}Sr$: 0.70376–0.70457, ε_{Ndt}: +6.8 to +2.7; Hogstad: $^{87}Sr/^{86}Sr$: 0.70537–0.70588, ε_{Ndt}: +2.1 to −0.5; Koldal: $^{87}Sr/^{86}Sr$: 0.70659–0.70911, ε_{Ndt}: +3.5 to −1.6) also indicate that in this sequence, parent magmas were characterized by a progressively more enriched Sr and Nd isotopic signature. In Løyning, the parent magma was slightly more magnesian and anorthitic than a primitive jotunite; in Hogstad, it is a primitive jotunite; and, in Koldal, an evolved jotunite. Given that plagioclase and orthopyroxene of the three intrusions display more differentiated compositions than the orthopyroxene and plagioclase megacryts of the enclosing anorthosites, it is suggested that the parent magmas of the small intrusions are residual melts after anorthosite formation which were entrained in the anorthositic diapir during its rise from lower crustal chambers.

Calculated densities of primitive jotunites (2.73–2.74 at FMQ, 0.15% H_2O, 200 ppm CO_2, 435 ppm F, 1150 °C, 3 kb) and evolved jotunites (2.75–2.76 at FMQ, 0.30% H_2O, 400 ppm CO_2, 870 ppm F, 1135 °C, 3 kb) demonstrate that they are much denser than the plagioclase of the surrounding anorthositic crystal mush (2.61–2.65). Efficient migration and draining of dense residual melts through the anorthositic crystal mush could have taken place along sloping floors (zones of lesser permeability in the mush), which occur along the margins of the rising anorthositic diapirs. This process takes into account the restricted occurrence of the mafic intrusions in the margins of the massif anorthosites. In a later stage, when the anorthosite was nearly consolidated, the residual melts were more differentiated (evolved jotunites) and could have been extracted into extensional fractures in the cooling and contracting anorthositic body in a similar way as aplitic dikes are emplaced in granitic plutons. As in the Rogaland Anorthositic Province, these dikes are much more abundant

* Corresponding author. Tel.: +32 4 3662253; fax: +32 4 3662921.
E-mail address: jvdauwera@ulg.ac.be (J. Vander Auwera).

0024-4937/$ - see front matter
doi:10.1016/j.lithos.2005.12.004

than the small mafic intrusions, collection and transport along dikes was probably more efficient than draining through the crystal mush.

Keywords: Proterozoic anorthosite; Jotunite; Ferrodiorite; Layered intrusion; Rogaland Anorthositic Province

1. Introduction

Consensus on the petrogenesis of Proterozoic massif-type anorthosites has not yet been reached, but many workers agree that their petrogenesis involves at least two major stages. The first stage involves crystallization of a mantle (e.g. Emslie, 1985) or crustal magma (e.g. Longhi et al., 1999; Longhi, 2005) emplaced at or near the base of the crust, which produces suspensions of plagioclase in evolved gabbroic liquids. In a second stage, these suspensions become gravitationally unstable and rise into the middle crust. Proterozoic massif-type anorthosites are characteristically associated with suites of rocks ranging in composition from basic (high-Al gabbros, jotunites (hypersthene-bearing monzodiorites), ferrodiorites) to intermediate (monzonites, mangerites) and acidic (quartz mangerites, charnockites). Although usually these suites of rocks are represented in minor volumes compared to the anorthosites, the debate about their origin has been active for more than 20 years and has helped constraining the petrology of Proterozoic anorthosites. A variety of hypotheses has been proposed to explain the origin of the basic rocks: they represent residual liquids after anorthosite crystallization (Ashwal, 1982; Morse, 1982; Wiebe, 1990; Emslie et al., 1994), they are products of partial melting of the lower crust (Duchesne et al., 1985; Longhi et al., 1999), they are immiscible liquids conjugated to mangerites (Philpotts, 1981), and they are the parental magmas of andesine anorthosite (Duchesne et al., 1974; Duchesne and Demaiffe, 1978; Demaiffe and Hertogen, 1981; Vander Auwera et al., 1998a; Longhi et al., 1999). Additionally, many workers ascribe the associated acidic rocks to melting of the lower crust (e.g. Emslie et al., 1994). Recent experimental and geochemical studies have shown, however, that it is possible to derive these evolved compositions by extensive fractionation of basic compositions (Owens et al., 1993; Vander Auwera et al., 1998a). In the Rogaland Anorthositic Province, the whole group of associated rocks has been referred to as the jotunite suite (Vander Auwera et al., 1998a). There, the least differentiated compositions (high MgO, low K_2O) of this suite outcrop as chilled margins of andesine anorthosite bodies (e.g. Hidra) and of the Bjerkreim-Sokndal layered intrusion (Duchesne, 1978; Duchesne and Hertogen, 1988; Wilson et al., 1996; Robins et al., 1997) (Fig. 1), whereas the more differentiated compositions occur essentially as dikes crosscutting the main intrusions. In variation diagrams, the chilled margins are distinct from the dikes and were referred to as "primitive" jotunites. More differentiated compositions (higher FeO, TiO_2 and P_2O_5) representing the starting compositions of the dike fractionation trend were referred to as "evolved" jotunites, differentiated from primitive jotunites by subtraction of a broadly leuconoritic cumulate (Vander Auwera et al., 1998a). Within the dikes, compositions range from evolved jotunites up to charnockites (Duchesne et al., 1985; Wilmart et al., 1989). Experimental data indicate that plausible parent magmas of the andesine anorthosite bodies (e.g. Hidra) and of the Bjerkreim-Sokndal intrusion are indeed jotunitic but slightly more magnesian and more anorthitic than the primitive jotunite experimentally studied by Vander Auwera and Longhi (1994) and Vander Auwera et al. (1998a) (Tjörn sample: TJ). The later stage of differentiation from evolved jotunites to charnockites occurred either within the dikes themselves or in a large magma chamber like Bjerkreim-Sokndal (Duchesne and Wilmart, 1997; Vander Auwera et al., 1998a; Wilson and Overgaard, 2005). The dikes may have been spawned by fractionation in an anorthositic intrusion or in a magma chamber like Bjerkreim-Sokndal (Vander Auwera et al., 1998a). Bolle et al. (2003) have assessed the Sr and Nd isotopic composition of the Rogaland jotunite suite. They showed that the primitive jotunites, the evolved jotunites and the acidic end-members of the suite are characterized by specific but partly overlapping Sr and Nd isotopic signatures: primitive jotunites: $^{87}Sr/^{86}Sr_{0.93Ga}$=0.704–0.707, ε_{Nd} (0.93 Ga)=+3.6 down to +1.2; evolved jotunites: $^{87}Sr/^{86}Sr_{0.93Ga}$=0.705–0.713, ε_{Nd} (0.93 Ga)=+0.4 down to −2.0; acidic end-members: $^{87}Sr/^{86}Sr_{0.93Ga}$=0.707–0.723, ε_{Nd} (0.93 Ga)=+1.4 down to −1.7. They thus proposed that fractionation from the primitive to the evolved jotunites and then to the charnockites involved crustal contamination.

In this paper, we present geochemical and isotopic data on three small mafic intrusions (Løyning, Hogstad, Koldal), which are typically enclosed in the marginal

zones of the Egersund-Ogna (Løyning, Koldal) and Åna-Sira (Hogstad) anorthosite bodies (Fig. 1). The purpose of this paper was to understand their connection with the enclosing anorthosites and more generally with the Rogaland jotunite suite, in order to bring additional constraints on the way anorthositic diapirs differentiate and crystallize. Using mineral compositions, geochemical and isotopic data, we will show that the parent magmas of these mafic intrusions range from primitive to evolved jotunites and represent residual melts after some anorthosite (leuconorite) fractionation and crustal contamination. Furthermore, their calculated densities are much higher than that of the plagioclase from the surrounding anorthositic crystal mush. We will then examine possible ways of extracting these residual liquids from the crystal mush during the final movements of the anorthositic diapir. We will suggest that draining of these residual dense liquids and their collection in small magma chambers were possible only when enough permeability was still available and on the sloping margins of the rising diapirs. This process takes into account the restricted occurrence of the small mafic intrusions in the marginal zones of the massif-type anorthosites. In a later stage, when the anorthositic diapir is nearly consolidated and has a brittle behavior, residual liquids are extracted in crosscutting dikes, which are widespread in the Rogaland anorthosites.

2. Geology of the Rogaland anorthositic complex

The Rogaland Anorthositic Province is one of the AMCG (Anorthosite–Mangerite–Charnockite–Granite) suites, which are characteristic of the Proterozoic (Ashwal, 1993). It consists of three large massif-type anorthosites (Egersund-Ogna, Håland-Helleren, Åna-Sira), a layered intrusion (Bjerkreim-Sokndal) and two smaller leuconoritic bodies (Hidra and Garsaknatt) (Fig. 1) (Michot, 1960; Michot and Michot, 1969). Contacts between these intrusions and the surrounding granulite facies gneisses are generally conformable. The Egersund-Ogna massif anorthosite is essentially made up of granulated homogeneous plagioclase with some megacrysts of high-Al orthopyroxene and plagioclase. The leuconoritic margin of the body is foliated, generally concordant with the foliation of the surrounding rocks (Marker et al., 2003). Two small mafic intrusions, Løyning and Koldal, have been identified within its southern margin. The Håland-Helleren massif consists of two distinct units: the Håland intrusion, a foliated anorthosite–leuconorite comparable to the foliated marginal zone of Egersund-Ogna body; the Helleren massif dominated by coarse-grained anorthosite (Michot, 1961). As shown by detailed mapping, the Åna-Sira intrusion is essentially made up of coarse-grained anorthosite and leuconorite (Krause and Pedall, 1980; Krause et al., 1985). It is characterized by Fe–Ti ore bodies, the Storgangen deposit and the Tellnes ilmenite–norite being the most important ones. Small intrusions like the Hogstad body are included in the anorthosite. The Bjerkreim-Sokndal layered intrusion comprises a lower part exhibiting a series of modally layered anorthosite–(leuco)norite–gabbronorite cumulates overlaid by essentially massive mangerites, quartz mangerites and charnockites (Michot, 1960, 1965; Duchesne et al., 1987a; Wilson et al., 1996; Duchesne and Wilmart, 1997). The acidic rocks extend southeastwards in an elongated body called the Apophysis (Demaiffe, 1972; Bolle, 1998). Layering in the Bjerkreim-Sokndal intrusion is deformed into a doubly plunging syncline, which southwards branches around the Åna-Sira anorthosite. This synformal structure has been explained by gravitational foundering (Paludan et al., 1994; Bolle et al., 2000, 2002). Jotunitic rocks mostly occur as dikes or small intrusions (i.e. Eia-Rekefjord, Hadland, Lomland, Tellnes, Varberg, Vaersland, Vettaland) crosscutting the massive anorthosites or form chilled margins of the leuconoritic bodies (Hidra and Garsaknatt) and the Bjerkreim-Sokndal intrusion (Demaiffe et al., 1973; Duchesne and Hertogen, 1988; Robins et al., 1997).

3. Field observations and petrography of the small mafic intrusions

The three mafic intrusions were emplaced in the marginal zones of the Egersund-Ogna (Løyning, Koldal) and Åna-Sira (Hogstad) massive anorthosites. The Løyning body (1250 m × 150 m) intruded into the foliated margin of the Egersund-Ogna anorthosite. Its contacts with the enclosing foliated anorthosite are sharp and concordant (Fig. 1). It has been subdivided in two subunits on the basis of the dominant lithologies (Fig. 2). The mafic to ultramafic lower unit consists of noritic, leuconoritic and locally, pyroxenitic layers several cm to several dm thick, showing a conspicuous magmatic layering dipping 70° southward and with an east–west direction. Small-scale modally graded layers indicate that the body has been slightly overturned. An olivine-bearing melanorite has been recognized close to the southern contact. There is a gradual transition towards the leuconorites of the upper unit. These leuconorites are homogeneous and differ from the Egersund-Ogna marginal zone by their non-foliated texture and finer grain size. At the northern contact,

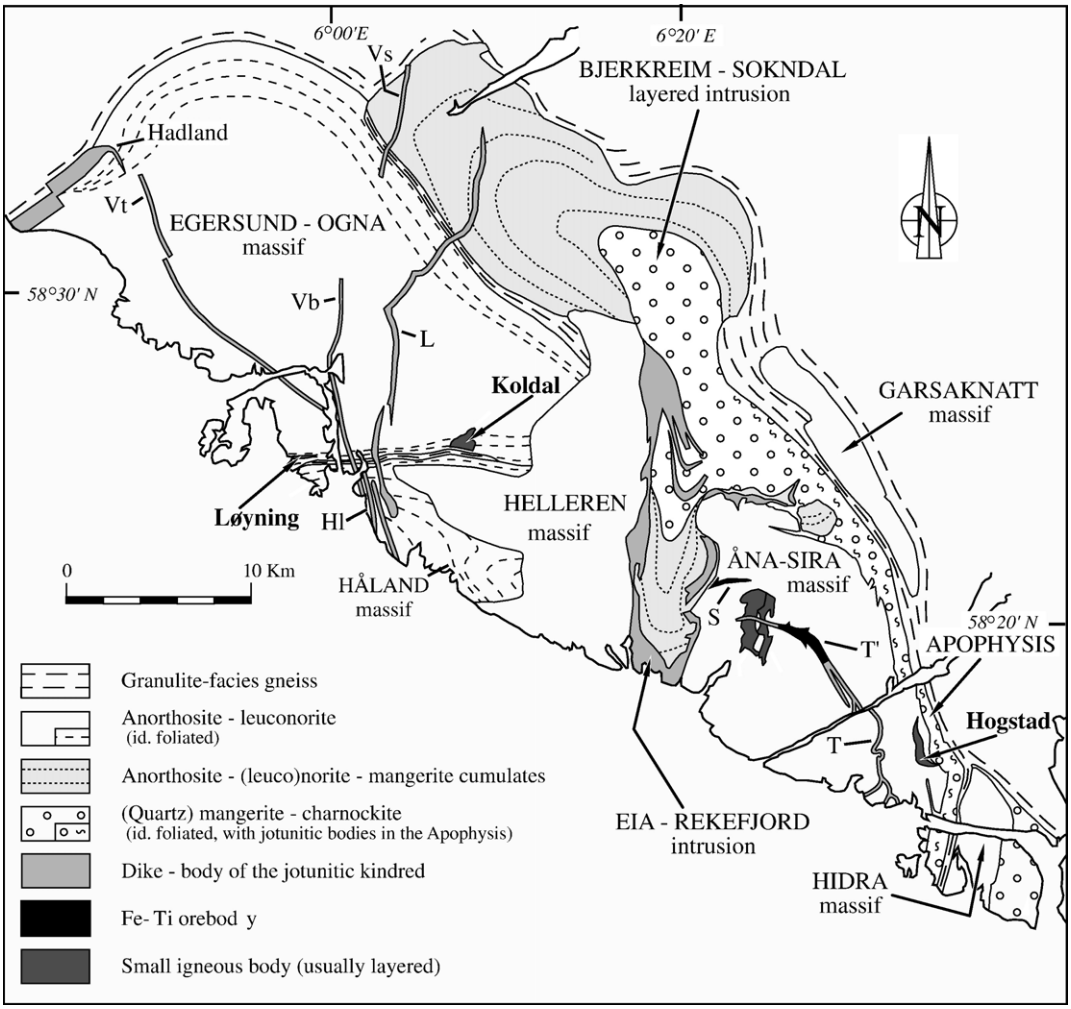

Fig. 1. The Rogaland Anorthosite Province (Michot, 1960; Michot and Michot, 1969; Rietmeijer, 1979; Wilmart, 1982; Duchesne et al., 1985, 1987a, b; Krause et al., 1985; Wilson et al., 1996; Bolle, 1998). Hl: Håland dike, L: Lomland dike, S: Storgangen deposit, T: Tellnes dike, T': Tellnes deposit, Vb: Varberg dike, Vt: Vettaland dike, Vs: Vaersland dike.

rather thin anorthositic dikes crosscut the upper unit and several leuconoritic dikes originating from the upper unit intrude the Egersund-Ogna anorthosite (Duchesne et al., 1991). Field and petrographic evidence indicate that the Løyning body has been deformed. A lineation is locally present and, in thin sections, the texture is granoblastic. Orthopyroxene and plagioclase are hypidiomorphic and plagioclase rims are usually reversely zoned (maximum 1.5% An). Olivine, orthopyroxene, plagioclase and ilmenite are always cumulus phases. Small amounts of anhedral clinopyroxene associated with orthopyroxene have been observed together with traces of sulphides (pyrite, chalcopyrite) and coronitic biotite surrounding ilmenite.

The noritic to leuconoritic Hogstad layered body (2 km × 200 m) intruded the eastern margin of the Åna-Sira anorthosite close to the contact with the Apophysis of the Bjerkreim-Sokndal intrusion (Fig. 1) (Boutefeu, 1973; Krause and Pedall, 1980; Castellani, 1993; Vander Auwera and Duchesne, 1996). The Hogstad body (Fig. 3) is crescent-shaped and has a maximum width in its central part and thins out towards its northern and southern extremities. The curvature goes from north–south in the northern end to east–west in the southern end. Based on the dominant lithologies, the intrusion has been subdivided into three subunits, which are from base to top: banded norites, mottled leuconorites and homogeneous gabbronorites (Fig. 3). A magmatic layering dipping 75° to 80° to the East is conspicuous in the banded norites and modal grading indicates that the top of the intrusion is to the East. Here too, field and petrographic evidence indicate

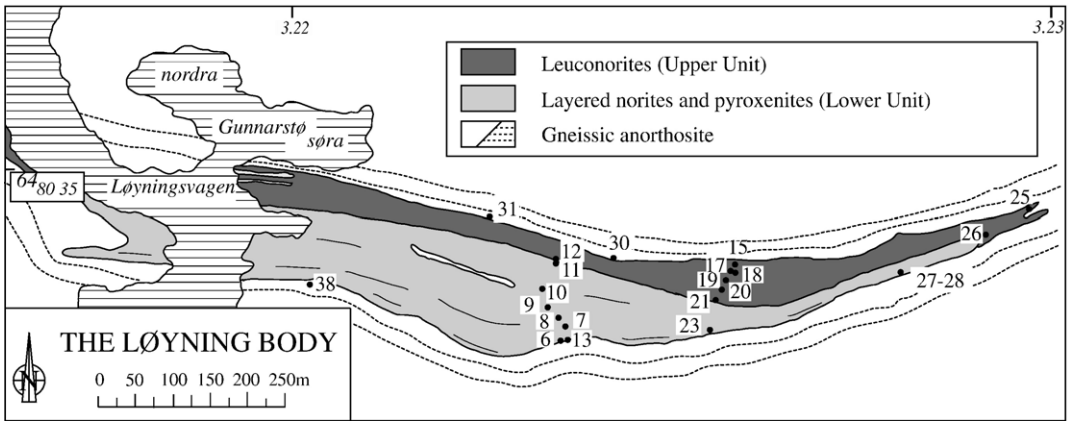

Fig. 2. Schematic geological map of the Løyning intrusion (Ernst, 1990; Ernst and Duchesne, 1991; Duchesne et al., 1991). Numbers correspond to sample location (e.g., 1 = GE-1) (UTM grid, zone 32 V). Samples GE-20, GE-30 and GE-31 are from anorthositic and leuconoritic dikes.

deformation: a subvertical lineation is locally present and plagioclase as well as orthopyroxene display granulated textures, bent twinning, kinks and ondulous extinction. The banded norites contain numerous inclusions of the Åna-Sira anorthosite ranging in size from 1 cm^2 up to 1500 m^2. A mottled leuconorite up to 70 m wide has been mapped in the center of the intrusion. Its width ranges from nought to 70 m in the central zone. It is characterized by oïkocrysts of orthopyroxene containing abundant inclusions of euhedral plagioclase. In sections perpendicular to the lineation, these oïkocrysts have a subcircular section

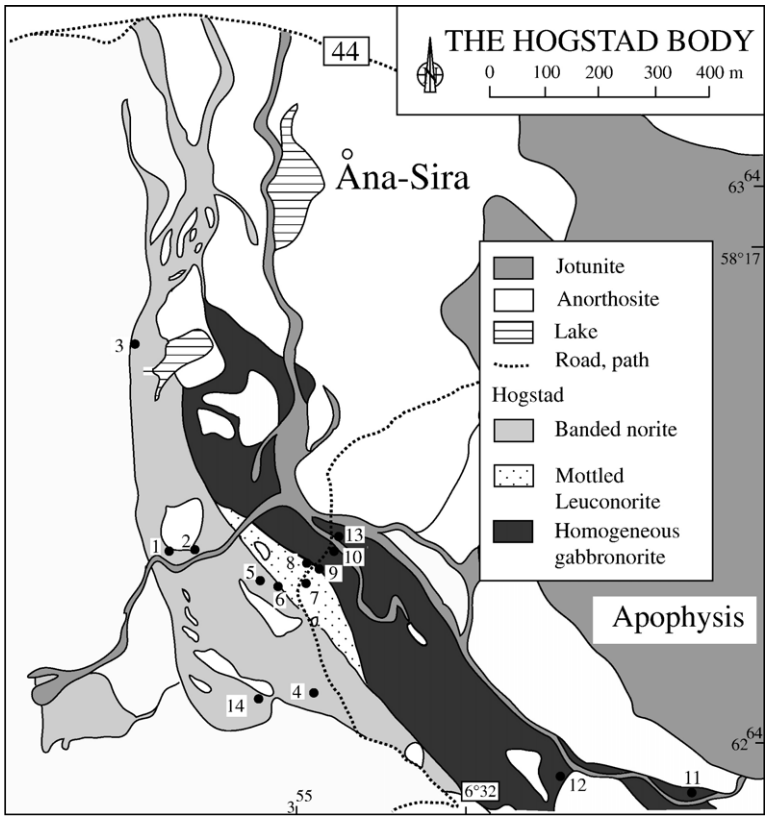

Fig. 3. Schematic geological map of the Hogstad intrusion modified after Boutefeu (1973), Castellani (1993) and Krause and Pedall (1980).

with a diameter of 2–3 cm. The transition from the mottled leuconorite to the homogeneous gabbronorites is marked by a leuconorite in which the proportion of mafic minerals rapidly increases upwards. The homogeneous gabbronorites are not banded but display a conspicuous igneous lamination. At the upper contact with the anorthosite, the lamination disappears and the grain size increases. Plagioclase, orthopyroxene and ilmenite are always cumulus phases. Magnetite, apatite and clinopyroxene are post-cumulus phases in the banded norites. Magnetite becomes cumulus in the mottled leuconorite and apatite as well as clinopyroxene, in the homogeneous gabbronorites. Traces of biotite and amphibole locally surround the Fe–Ti oxides.

The Koldal body is emplaced in the southern foliated margin of the Egersund-Ogna anorthosite, about 6 km to the East of the Løyning intrusion (Figs. 1 and 4). At Koldal, the Egersund-Ogna anorthosite displays a subvertical foliation and is in contact with a 150 m wide septum of migmatitic gneisses. The intrusion is essentially made of layered norites and leuconorites but a mangeritic unit has been observed in two localities (Fig. 4). The layering is subvertical with a generally E–W direction. Since a well-developed magmatic layering is only observed in the norites, a detailed stratigraphy of the body has not been realized. The southern contact between Koldal and the surrounding anorthosite is subvertical and concordant with the layering. On the contrary, in the northwestern part, the roof of the intrusion crosscuts the foliated anorthosite and dips 30° to the north. The norites contain hypidiomorphic, locally antiperthitic plagioclase, inverted pigeonite, augite, hemoilmenite, magnetite and apatite. Augite is not abundant, usually interstitial or occurring as exsolutions granules in the inverted pigeonite. The leuconorites have a similar mineralogical composition with a lesser amount of inverted pigeonite and no apatite. The mangerites contain large crystals of mesoperthite associated with smaller grains of ortho- and clinopyroxene as well as antiperthitic plagioclase. Ilmenite, magnetite and apatite are also present. The influence of deformation is conspicuous in the bent twinning, undulous extinction and granulation of minerals. A meter-thick jotunitic dike intruded the anorthosite close to the contact with Koldal (samples 89-25 and 89-26) and is parallel to the contact (not shown on Fig. 4).

These field and petrographic data indicate that the cumulus sequence in the three intrusions is similar to what has been described in the nearby Bjerkreim-Sokndal intrusion. Indeed, in macrocyclic unit IV of Bjerkreim-Sokndal, troctolitic cumulates are overlaid by ilmenite norites, magnetite norites and apatite-bearing gabbronorites corresponding respectively to the

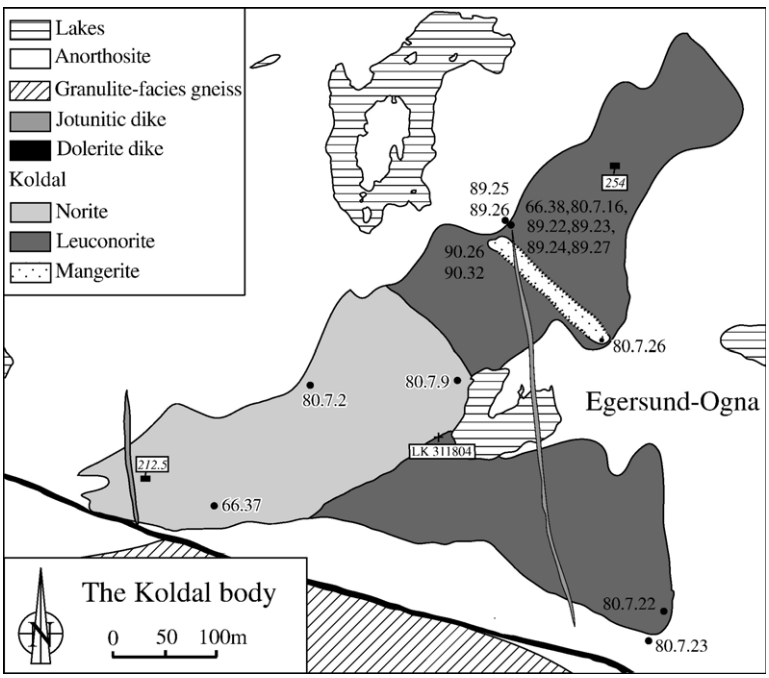

Fig. 4. Schematic geological map of the Koldal intrusion. Italic numbers correspond to topographic heights (Point LK 311804 in UTM grid, zone 32 V). The extension of the mangerite unit has been extrapolated between the two observation points.

appearance of cumulus magnetite, then simultaneous appearance of cumulus clinopyroxene and apatite (e.g. Wilson et al., 1996). Moreover, layers of mangerite with cumulus mesoperthites occur above gabbronoritic layers in the Bjerkreim-Sokndal intrusion (Wilson et al., 1996; Duchesne and Wilmart, 1997).

Significant features of these three intrusions are the subvertical orientation of their layering as well as evidence of subsolidus deformation. Vertical layering has been described in undeformed layered intrusions such as the Skaergaard (Wager and Brown, 1968), and this raises the possibility that the present orientation of the layering in Løyning, Hogstad and Koldal is original. Nevertheless, in the Skaergaard, textures observed in zones with vertical layering are less regular than those observed in zones with horizontal layering (B. Robins, pers. comm.). Additionally, the conspicuous evidence of subsolidus deformation in the three small intrusions suggests that layering developped horizontally and then tilted into subvertical position or even slightly overturned. Given that these intrusions are all included in massif-type anorthosites, the simplest explanation for this tilting is to be found in the final movements of the anorthositic diapirs. In support of this hypothesis, there are several examples of well-preserved layering after deformation of the intrusion. In the nearby Bjerkreim-Sokndal body, cumulates display a penetrative foliation S_1 and a mineral lineation L_1, overprinting the original igneous layering S_0 (Paludan et al., 1994; Bolle et al., 2002), which are linked to the syn- to post-magmatic folding event which gave rise to the Bjerkreim-Sokndal syncline. In the Stillwater Complex, layered rocks are steeply dipping and this disposition has led to the interpretation that the intrusion crystallized horizontally and was then tilted by later tectonic movements (Jones et al., 1960). We thus admit that the subvertical position of the layering in Løyning and Hogstad was acquired during late movements of the diapir when these intrusions were fully crystallized. In the case of Koldal, the observations are more difficult to interpret as its southern contact is concordant with the foliated anorthosite and its northern contact, discordant. This latter observation implies that Koldal intruded the already foliated anorthosite. Then, it is possible that only its southern part was vertically tilted by shearing along a localized zone of the diapir parallel with the anorthosite foliation.

As previously mentioned, the Hogstad intrusion is located within the eastern margin of the Åna-Sira anorthosite close to the Apophysis of the Bjerkreim-Sokndal intrusion (Fig. 1). The Apophysis is a foliated, sheet-like intrusion made of jotunites, mangerites and charnockites that show evidence of mingling and possibly mixing at various scale (Demaiffe, 1972; Duchesne et al., 1987b; Bolle, 1996). Given the close proximity of Hogstad and the Apophysis, a possible relationship between both intrusions is briefly explored here. Detailed mapping by Bolle (1998) (see also Marker, 2003) has shown that the Apophysis contains inclusions from the Åna-Sira anorthosite and that during its emplacement, it has sent offshoots within the surrounding rocks, Åna-Sira on its western side and the high grade gneisses on its eastern side. These observations demonstrate the intrusive character of the Apophysis and indicate that emplacement of the Apophysis took place when the margin of the Åna-Sira anorthosite, and thus Hogstad, were fully consolidated. The parent magma of Hogstad is thus probably not derived from the Apophysis. This conclusion is also supported by the lack of acid compositions in Hogstad. Indeed, these are quite abundant in the Apophysis and, if magmas of the Hogstad intrusion were derived from the Apophysis, we would expect the same range of composition in both intrusions.

The age of the small intrusions has not been directly measured. Nevertheless, given the above discussion about the origin of the vertical layering, we accept that these small magma chambers were penecontemporaneous with the anorthosites and have thus the same age as the main period of magmatism. Emplacement ages of 930 Ma have been reported for zircons included in the orthopyroxene megacrysts of the anorthosites and a quartz mangerite from the Tellnes dike (Schärer et al., 1996). In the following, initial Sr isotopic compositions and ε_{Ndt} have thus been calculated at 930 Ma. It is also worth noting that field evidence and precise geochronological data have not revealed repeated cycles of magmatism within the Rogaland anorthositic complex. Indeed, these data indicate that the Sveconorwegian regional metamorphism (M1: ca. 1.02–1.00 Ga, 6–8 kbar: Pasteels and Michot, 1975; Wielens et al., 1981; Bingen et al., 1993; Bingen and van Breemen, 1998; Möller et al., 2003, 2002) was followed by a thermal event (M2: 930 Ma) associated with intrusion of the Rogaland anorthositic complex and dated directly on the Rogaland intrusion (Schärer et al., 1996) and on the associated augen gneisses (Bingen and van Breemen, 1998). Regional decompression to 5.6 kbar (SHRIMP U–Pb zircon age: Tomkins et al., 2005) was recently reported at 955 Ma, whereas progressive reequilibration of higher grade metamorphic assemblages during cooling (retrograde M3) was dated at 908 Ma (Möller et al., 2003).

4. Geochemistry

4.1. Methods

Magnetite, ilmenite, apatite and pyroxenes were separated from a selection of samples from Hogstad using classical mineral separation techniques (Frantz magnetic separator, heavy liquids).

Mineral compositions were analyzed with a CAMECA electron microprobe (CAMST, Université Catholique de Louvain, Belgium) equipped with a wavelength dispersive system. Mineral standards were used for calibration and X-ray intensities were reduced using the Cameca PAP correction program. Results are given in Tables 1–3 and Fig. 5.

Whole-rock samples and mineral separates were analyzed for major and some trace elements by X-ray fluorescence on a CGR Lambda 2020 Spectrometer at the University of Liège (analyst G. Bologne) (Bologne and Duchesne, 1991). Major elements were analyzed on Li borate glass discs. Depending on the elements, the accuracy ranges between 0.5% and 3.1%. Na and some trace elements (see Tables 4 and 8) were analyzed on pressed powder pellets with an accuracy between 5% and 12% (Bologne and Duchesne, 1991). The other trace elements were analyzed on a VG elemental PQ2 Plus inductively coupled plasma-mass spectrometer at the University of Liège (Vander Auwera et al., 1998b). Whole rocks are prepared using a lithium metaborate fusion, whereas mineral separates are prepared using an open acid digestion. Calibration of the ICP-MS is made with international reference materials and the accuracy is better than 10%. Major and trace element data are presented in Tables 4–8.

Samples were selected for Sr and Nd isotopic analyses to encompass the entire range of major and trace element compositions. The chemical procedures used are based on those initially described in Weis and Frey (1991), except that the samples here did not need to be leached. Duplicates were processed through the whole chemical procedure and are all within analytical error. Total blank values were $\ll 1$ ng for each isotopic system considered, which is negligible with respect to the abundance of the elements in the dissolved samples (i.e. >16,000 and 7000 ng on average for Sr and Nd). Isotopic measurements were performed at the Université Libre de Bruxelles and at the University of British Columbia. Sr and Nd isotopic ratios were normalized to $^{86}Sr/^{88}Sr = 0.1194$ and $^{146}Nd/^{144}Nd = 0.7219$, respectively. In Brussels, Sr and Nd isotopic compositions were measured on a Micromass VG Elemental Sector 54 multicollector thermal ionization mass spectrometer. Sr and Nd isotopic compositions were measured in the dynamic mode on a single Ta and triple Re–Ta filament, respectively. The average $^{87}Sr/^{86}Sr$ of the NBS 987 and $^{143}Nd/^{144}Nd$ of the Rennes Nd standard (Chauvel and Blichert-Toft, 2001) during the period of our analyses were 0.710271 ± 7 ($2\sigma_m$ on 12 measurements) and 0.511961 ± 11 ($2\sigma_m$ on 7 measurements), respectively. In Vancouver, the analyses were carried out on a Triton multicollector thermal ionization mass spectrometer. Sr and Nd compositions were measured in the dynamic mode on a single Ta and double Re–Ta filament, respectively. The average $^{87}Sr/^{86}Sr$ of the NBS 987 standard and $^{143}Nd/^{144}Nd$ of the La Jolla Nd standard during the period of our analyses were 0.710255 ± 10 ($2\sigma_m$ on 20 measurements) and 0.511854 ± 8 ($2\sigma_m$ on 7 measurements), respectively. Duplicates of the same sample measured in the two laboratories are in agreement within error. Results are shown in Table 9.

4.2. Chemical and isotopic cryptic layering

Despite the small size (0.19 to 0.63 km^2) of the three mafic intrusions, their mineral and isotopic compositions display some cryptic layering (Figs. 6–8). From the base to the top of Løyning (Fig. 6), the An content of plagioclase increases up to a maximum value of An_{59} (GE-23), then steadily decreases from samples GE-23 to GE-9. Somewhere between samples GE-9 and GE-10, plagioclase composition becomes again more calcic. The transition between the Lower and Upper Units is underlined by a sharp decrease in An content. Plagioclase composition then remains rather constant up to the top of the intrusion. Moreover, in the olivine-bearing melanorites (Lower Unit), plagioclase has no exsolution and then becomes increasingly antiperthitic upwards. Orthopyroxene compositional variations are more restricted. The Mg# increases slightly from the base up to sample GE-23, then remains constant. It decreases from samples GE-8 to GE-9 and then increases up to the top of the Lower Unit. Contrary to what is observed for plagioclase, pyroxene composition remains constant at the transition between the two units. The hematite content of ilmenite ranges from below 9% at the base up to 18% at the top of the intrusion (not shown on Fig. 6). Initial Sr isotopic compositions calculated back to 930 Ma range from 0.70376 to 0.70457 and ε_{Ndt} from +6.2 to +2.7. Within the Lower Unit, the maximum value of Sr_i is found, as expected, with plagioclase displaying the lowest An content. At the transition between the Lower and Upper Units, Sr_i remains nearly constant, but ε_{Ndt} increases dramatically. Leuconoritic (GE30, GE31) and anorthositic (GE20)

Table 1
Microprobe analyses of feldspars

Massif	Sample #	*n*	SiO_2	TiO_2	Al_2O_3	FeO	MgO	MnO	CaO	K_2O	Na_2O	Total	Si	Ti	Al	Fe	Mg	Mn	Ca	K	Na	∑Cations	Ab	Or	An
Løyning	GE-6		55.56	0.02	26.93	0.06	0.01	0.05	9.22	1.28	5.46	98.59	2.542	0.001	1.452	0.002	0.001	0.002	0.452	0.074	0.484	5.010	47.9	7.4	44.7
	GE-7		54.61	0.04	27.80	0.21	0.00	0.00	10.04	0.73	5.33	98.76	2.496	0.001	1.498	0.008	0.000	0.000	0.492	0.043	0.473	5.011	46.9	4.2	48.8
	GE-8		53.81	0.09	27.93	0.15	0.03	0.01	10.10	0.89	5.42	98.43	2.474	0.003	1.514	0.006	0.002	0.000	0.498	0.052	0.483	5.032	46.8	5.0	48.2
	GE-9		56.54	0.04	26.24	0.07	0.01	0.03	7.95	1.03	6.38	98.29	2.585	0.001	1.414	0.003	0.001	0.001	0.389	0.060	0.565	5.019	55.7	5.9	38.4
	GE-10		54.38	0.04	27.64	0.13	0.01	0.04	10.05	0.86	5.29	98.44	2.496	1.495	0.001	0.005	0.000	0.002	0.494	0.050	0.471	5.014	46.4	5.0	48.7
	GE-11		54.29	0.03	28.00	0.13	0.03	0.05	10.37	0.52	5.45	98.87	2.481	0.001	1.508	0.005	0.002	0.002	0.508	0.030	0.483	5.020	47.3	3.0	49.7
	GE-12		56.86	0.03	26.54	0.21	0.00	0.00	8.47	0.58	6.52	99.21	2.575	0.001	1.417	0.008	0.000	0.000	0.411	0.034	0.572	5.018	56.3	3.3	40.4
	GE-15		56.29	0.11	26.11	0.19	0.06	0.00	8.07	0.60	6.60	98.03	2.579	0.004	1.410	0.007	0.004	0.000	0.396	0.035	0.586	5.021	57.6	3.4	38.9
	GE-17		56.28	0.00	26.24	0.11	0.01	0.00	8.27	0.52	6.72	98.15	2.576	0.000	1.416	0.004	0.001	0.000	0.406	0.031	0.597	5.031	57.8	3.0	39.3
	GE-18		57.35	0.07	25.82	0.19	0.02	0.03	8.00	0.49	6.77	98.74	2.605	0.002	1.382	0.007	0.001	0.001	0.390	0.029	0.596	5.013	58.8	2.8	38.4
	GE-19		56.45	0.03	26.51	0.10	0.01	0.02	8.56	0.62	6.37	98.67	2.570	0.001	1.423	0.004	0.001	0.001	0.417	0.036	0.563	5.016	55.4	3.5	41.1
	GE-21		56.06	0.08	26.82	0.16	0.01	0.00	8.74	0.75	6.43	99.05	2.550	0.003	1.437	0.006	0.001	0.000	0.426	0.044	0.567	5.034	54.7	4.2	41.1
	GE-23		51.80	0.06	29.85	0.17	0.00	0.00	12.25	0.12	4.60	98.85	2.377	1.615	0.002	0.006	0.000	0.000	0.602	0.007	0.409	5.018	40.2	0.7	59.1
	GE-30		57.21	0.00	25.69	0.23	0.00	0.05	8.04	0.54	6.62	98.38	2.609	0.000	1.381	0.009	0.000	0.002	0.393	0.031	0.585	5.010	58.0	3.1	38.9
	GE-38		53.57	0.00	28.67	0.25	0.00	0.00	10.91	0.30	5.20	98.90	2.449	0.000	1.545	0.009	0.000	0.000	0.534	0.017	0.461	5.015	45.5	1.7	52.8
Hogstad	1	3	56.88	0.02	27.56	0.19	0.01	0.01	9.53	0.56	5.97	100.74	2.541	0.001	1.451	0.007	0.001	0.001	0.457	0.032	0.517	5.007	51.4	3.2	45.4
	2	3	56.71	0.01	27.26	0.13	0.01	0.01	9.09	0.60	6.00	99.82	2.553	0.000	1.446	0.005	0.001	0.000	0.439	0.034	0.524	5.002	52.6	3.4	44.0
	3	3	55.78	0.02	27.16	0.14	0.01	0.02	9.28	0.31	6.26	98.98	2.536	0.001	1.455	0.005	0.001	0.001	0.452	0.018	0.552	5.020	54.0	1.7	44.3
	5	4	55.97	0.03	27.19	0.11	0.01	0.01	9.46	0.73	5.86	99.37	2.538	0.001	1.453	0.005	0.001	0.000	0.459	0.043	0.515	5.014	50.7	4.2	45.2
	6	3	57.59	0.02	26.77	0.14	0.00	0.03	9.00	0.69	6.20	100.44	2.577	0.000	1.412	0.005	0.000	0.001	0.432	0.040	0.538	5.005	53.3	3.9	42.8
	7	6	56.70	0.04	27.49	0.19	0.03	0.00	9.54	0.53	5.90	100.43	2.541	0.001	1.452	0.007	0.002	0.000	0.458	0.030	0.513	5.004	51.2	3.0	45.8
	9	4	57.31	0.05	26.45	0.15	0.01	0.01	8.80	0.65	6.19	99.62	2.584	0.002	1.406	0.006	0.001	0.001	0.425	0.038	0.541	5.001	53.9	3.7	42.4
	10	3	57.60	0.03	26.35	0.12	0.00	0.04	8.33	0.87	6.31	99.66	2.595	0.001	1.399	0.004	0.000	0.002	0.402	0.050	0.551	5.005	54.9	5.0	40.1
	11	4	57.45	0.01	26.14	0.08	0.01	0.00	8.27	0.57	6.63	99.17	2.599	0.001	1.394	0.003	0.001	0.000	0.401	0.033	0.582	5.011	57.3	3.2	39.5
	12	3	59.07	0.02	26.05	0.05	0.01	0.01	7.81	0.85	6.93	100.80	2.626	0.001	1.366	0.002	0.001	0.000	0.372	0.048	0.597	5.014	58.7	4.7	36.6
Koldal	66.37		55.39	0.03	26.90	0.25	0.00	0.01	8.85	0.49	5.92	97.84	2.543	0.001	1.456	0.010	0.000	0.001	0.436	0.029	0.527	5.002	53.2	2.9	43.9
	66.38		57.34	0.06	26.28	0.07	0.00	0.01	7.84	0.68	6.61	98.89	2.598	0.002	1.403	0.003	0.000	0.000	0.381	0.040	0.580	5.006	58.0	4.0	38.1
	80.7.2		57.13	0.08	26.63	0.21	0.00	0.00	8.20	0.79	6.44	99.48	2.580	0.003	1.417	0.008	0.000	0.000	0.397	0.045	0.564	5.013	56.0	4.5	39.5
	80.7.16		56.89	0.11	26.73	0.19	0.00	0.06	8.41	0.48	6.16	99.03	2.573	0.004	1.425	0.007	0.000	0.002	0.407	0.028	0.540	4.986	55.4	2.8	41.8
	80.7.22		56.02	0.09	26.61	0.18	0.00	0.04	8.07	0.51	6.33	97.85	2.567	0.003	1.437	0.007	0.000	0.002	0.396	0.030	0.562	5.004	56.9	3.0	40.1
	80.7.23	Core	56.20	0.02	26.47	0.20	0.00	0.00	7.86	0.57	6.34	97.66	2.579	0.001	1.432	0.008	0.000	0.000	0.386	0.033	0.564	5.003	57.3	3.4	39.3
		Core	56.42	0.07	26.71	0.19	0.00	0.00	8.25	0.53	6.16	98.33	2.572	0.003	1.435	0.007	0.000	0.000	0.403	0.031	0.544	4.995	55.7	3.2	41.2
		Rim	55.77	0.05	27.24	0.16	0.00	0.05	8.79	0.54	5.94	98.54	2.543	0.002	1.463	0.006	0.000	0.002	0.430	0.032	0.525	5.002	53.2	3.2	43.6
	80.7.26		59.63	0.15	21.41	0.31	0.19	0.05	2.88	7.54	4.49	96.65	2.799	0.006	1.185	0.012	0.013	0.002	0.145	0.452	0.409	5.022	40.6	45.0	14.4
		Exsolved Kspar	61.64	0.00	18.84	0.13	0.00	0.04	0.05	14.58	1.03	96.31	2.951	0.000	1.063	0.005	0.000	0.002	0.003	0.891	0.096	5.010	9.7	90.1	0.3
		Host plag	59.43	0.07	24.78	0.09	0.00	0.00	6.01	0.14	7.79	98.31	2.685	0.002	1.320	0.003	0.000	0.000	0.291	0.008	0.682	4.992	69.5	0.8	29.7
			59.14	0.04	24.77	0.15	0.00	0.00	5.88	0.30	7.65	97.93	2.686	0.002	1.326	0.006	0.000	0.000	0.286	0.017	0.674	4.995	69.0	1.8	29.3

For Hogstad, compositions are given as the average of *n* analyses. For Løyning, selected analyses are close to the calculated average for each sample. In Koldal, sample 80.7.23 is from the surrounding anorthosite.

Table 2
Selected microprobe analyses of pyroxenes

Massif	Sample #		SiO_2	TiO_2	Al_2O_3	FeOt	MgO	MnO	CaO	Na_2O	Total	Si	Ti	Al	Fe	Mg	Mn	Ca	Na	∑Cations	Wo	En	Fs
Løyning	GE-6	opx	51.50	0.22	1.97	22.05	23.26	0.28	0.62	0.00	99.90	1.905	0.007	0.087	0.685	1.283	0.009	0.024	0.000	4.000	1.2	64.1	34.2
	GE-7	opx	51.79	0.26	2.31	20.38	23.35	0.25	1.11	0.02	99.47	1.913	0.007	0.113	0.632	1.285	0.018	0.044	0.002	4.014	2.2	64.9	31.9
	GE-8	opx	52.01	0.31	2.51	20.35	23.44	0.33	1.17	0.04	100.16	1.912	0.009	0.108	0.627	1.293	0.011	0.046	0.002	4.008	2.3	65.4	31.7
	GE-9	opx	51.86	0.28	1.77	22.16	21.92	0.36	1.05	0.00	99.40	1.938	0.009	0.079	0.694	1.222	0.011	0.043	0.000	3.996	2.2	62.0	35.2
	GE-10	opx	51.56	0.29	2.22	21.49	22.82	0.30	1.12	0.02	99.82	1.909	0.009	0.098	0.668	1.259	0.009	0.045	0.002	3.999	2.3	63.6	33.7
	GE-11	opx	51.36	0.26	2.55	19.48	23.61	0.31	1.19	0.03	98.79	1.908	0.007	0.102	0.607	1.307	0.009	0.047	0.002	3.989	2.4	66.3	30.8
	GE-12	opx	51.74	0.41	2.42	20.59	24.47	0.24	0.66	0.02	100.55	1.887	0.011	0.103	0.634	1.331	0.007	0.026	0.002	4.001	1.3	66.6	31.7
	GE-15	opx	51.92	0.19	1.42	21.03	23.40	0.29	0.71	0.00	98.96	1.924	0.004	0.062	0.657	1.292	0.009	0.029	0.000	3.977	1.5	65.0	33.1
	GE-17	opx	52.04	0.24	1.60	20.12	24.25	0.21	0.82	0.02	99.30	1.876	0.006	0.067	0.619	1.304	0.006	0.032	0.002	3.912	1.6	66.5	31.6
	GE-19	opx	51.81	0.17	2.08	19.87	24.02	0.21	0.74	0.01	98.91	1.921	0.004	0.091	0.619	1.328	0.007	0.029	0.000	3.999	1.5	67.0	31.2
	GE-21	opx	50.88	0.31	2.29	19.85	24.20	0.28	0.75	0.01	98.57	1.890	0.009	0.100	0.62	1.339	0.009	0.029	0.000	3.996	1.5	67.1	31.0
	GE-23	opx	51.41	0.32	2.71	20.81	23.57	0.22	1.18	0.06	100.28	1.887	0.009	0.117	0.641	1.289	0.007	0.046	0.004	4.000	2.3	65.0	32.3
	GE-30	opx	50.81	0.22	1.25	26.12	20.55	0.38	0.82	0.02	100.17	1.912	0.007	0.057	0.825	1.153	0.011	0.034	0.002	4.001	1.7	57.0	40.8
	GE-38	opx	51.57	0.23	1.52	22.32	22.59	0.27	0.84	0.02	99.36	1.924	0.007	0.067	0.7	1.256	0.009	0.034	0.002	3.999	1.7	62.8	35.0
Hogstad	1	cpx	51.18	0.43	2.53	9.65	12.86	0.17	22.28	0.52	99.62	1.917	0.012	0.112	0.302	0.718	0.005	0.894	0.038	3.998	46.6	37.4	15.7
	1	opx	52.29	0.20	1.36	23.69	21.30	0.45	0.80	0.04	100.13	1.956	0.006	0.060	0.741	1.188	0.014	0.032	0.003	4.000	1.6	60.2	37.5
	2	cpx	51.01	0.52	2.66	10.89	13.23	0.19	20.03	0.50	99.03	1.925	0.015	0.118	0.343	0.744	0.006	0.810	0.037	3.998	42.6	39.1	18.0
	2	opx	52.24	0.19	1.50	22.97	21.57	0.41	0.92	0.04	99.85	1.954	0.005	0.066	0.718	1.203	0.013	0.037	0.003	3.999	1.9	61.0	36.4
	3	cpx	50.51	0.56	2.68	10.08	13.11	0.20	21.04	0.55	98.72	1.909	0.016	0.119	0.318	0.738	0.006	0.852	0.040	3.998	44.5	38.6	16.6
	3	opx	51.72	0.20	1.52	21.67	21.04	0.47	2.20	0.09	98.91	1.950	0.006	0.067	0.684	1.182	0.015	0.089	0.007	4.000	4.5	60.0	34.7
	5	cpx	50.77	0.47	2.75	9.24	13.17	0.21	21.51	0.52	98.64	1.917	0.013	0.123	0.291	0.741	0.007	0.870	0.038	4.000	45.6	38.8	15.2
	5	opx	52.19	0.12	1.54	22.02	22.12	0.42	0.76	0.02	99.17	1.957	0.003	0.068	0.691	1.236	0.013	0.030	0.001	3.999	1.5	62.7	35.1
	6	cpx	51.94	0.41	2.41	11.47	13.34	0.17	19.60	0.49	99.82	1.948	0.011	0.107	0.36	0.746	0.005	0.788	0.036	4.001	41.5	39.3	19.0
	6	opx	52.26	0.14	1.26	23.86	21.05	0.45	0.70	0.04	99.75	1.965	0.004	0.056	0.75	1.180	0.014	0.028	0.003	4.000	1.4	59.8	38.0
	7	cpx	51.69	0.43	2.57	9.78	12.67	0.25	21.85	0.50	99.74	1.937	0.012	0.114	0.307	0.708	0.008	0.877	0.037	4.000	46.2	37.3	16.2
	7	opx	52.28	0.17	1.35	23.99	20.59	0.45	0.65	0.00	99.47	1.972	0.005	0.060	0.757	1.157	0.014	0.026	0.000	3.991	1.3	59.2	38.7
	9	cpx	51.62	0.39	2.29	9.94	13.09	0.21	21.34	0.53	99.40	1.939	0.011	0.101	0.312	0.733	0.007	0.859	0.038	4.000	45.0	38.4	16.3
	9	opx	52.24	0.19	1.28	22.74	21.09	0.42	0.97	0.10	99.04	1.972	0.005	0.057	0.718	1.186	0.013	0.039	0.007	3.997	2.0	60.6	36.7
	10	cpx	51.06	0.46	2.38	13.87	12.80	0.29	19.39	0.50	100.75	1.910	0.013	0.105	0.434	0.714	0.009	0.777	0.036	3.998	40.2	36.9	22.4
	10	opx	51.71	0.17	1.28	25.70	19.26	0.42	0.82	0.02	99.37	1.971	0.005	0.057	0.819	1.095	0.014	0.033	0.001	3.995	1.7	55.8	41.8
	11	opx	50.45	0.10	1.17	28.96	17.01	0.56	0.90	0.01	99.15	1.961	0.003	0.053	0.941	0.986	0.018	0.037	0.001	4.000	1.9	49.7	47.5
	12	cpx	51.52	0.46	2.17	12.58	11.96	0.34	20.55	0.50	100.08	1.943	0.013	0.096	0.397	0.672	0.011	0.830	0.037	3.999	43.5	35.2	20.8
	12	opx	51.16	0.17	1.23	28.23	17.73	0.62	0.91	0.02	100.07	1.962	0.005	0.055	0.906	1.013	0.020	0.037	0.002	4.000	1.9	51.3	45.9
Koldal	66.37	opx	50.80	0.06	1.13	25.54	20.22	0.57	0.62	0.00	98.94	1.949	0.002	0.051	0.820	1.157	0.019	0.026	0.000	4.023	1.3	57.2	41.5
		cpx	50.06	0.37	1.92	10.21	13.33	0.27	21.59	0.25	98.00	1.922	0.011	0.087	0.328	0.763	0.009	0.888	0.019	4.027	44.7	38.4	16.9
	66.38	cpx	50.20	0.23	1.63	11.26	11.84	0.24	21.46	0.31	97.17	1.953	0.007	0.075	0.366	0.687	0.008	0.894	0.023	4.013	45.7	35.1	19.1
		opx	50.43	0.16	1.10	27.53	17.36	0.65	0.78	0.00	98.01	1.973	0.005	0.051	0.901	1.013	0.022	0.033	0.000	3.996	1.7	51.5	46.9
	80.7.2	cpx	50.22	0.38	2.05	11.20	12.24	0.35	21.53	0.01	97.98	1.936	0.011	0.093	0.361	0.703	0.012	0.889	0.001	4.006	45.3	35.8	19.0
		opx	50.55	0.15	1.07	26.70	18.18	0.81	0.74	0.00	98.20	1.967	0.005	0.049	0.869	1.055	0.027	0.031	0.000	4.001	1.6	53.2	45.2
	80.7.22	cpx	50.81	0.29	1.90	9.85	13.41	0.30	21.24	0.37	98.17	1.942	0.008	0.086	0.315	0.764	0.010	0.869	0.028	4.021	44.4	39.0	16.6
		opx	51.42	0.19	0.83	23.71	21.49	0.55	0.57	0.00	98.76	1.958	0.005	0.037	0.755	1.220	0.018	0.023	0.000	4.016	1.2	60.5	38.3
	80.7.16	opx	50.83	0.08	0.84	27.58	18.84	0.55	0.68	0.00	99.40	1.960	0.002	0.038	0.889	1.083	0.018	0.028	0.000	4.018	1.4	53.6	45.0
		cpx	50.54	0.28	1.87	11.93	12.48	0.31	20.99	0.33	98.73	1.938	0.008	0.085	0.383	0.713	0.010	0.862	0.025	4.023	43.8	36.2	20.0
	80.7.23	opx	52.30	0.15	1.32	20.46	24.35	0.32	0.49	0.00	99.39	1.944	0.004	0.058	0.636	1.349	0.010	0.020	0.000	4.020	1.0	67.0	32.1
		cpx	50.67	0.41	2.17	7.67	14.31	0.17	22.42	0.07	97.89	1.926	0.012	0.097	0.244	0.811	0.005	0.913	0.005	4.014	46.3	41.1	12.6
	80.7.26	cpx	50.57	0.41	1.54	11.60	12.60	0.40	20.39	0.49	98.00	1.948	0.012	0.070	0.374	0.724	0.013	0.842	0.037	4.018	43.1	37.1	19.8
		opx	50.54	0.17	0.76	27.75	18.30	0.73	0.63	0.00	98.88	1.962	0.005	0.035	0.901	1.059	0.024	0.026	0.000	4.012	1.3	52.7	46.0

In Koldal, sample 80.7.23 is from the surrounding anorthosite.

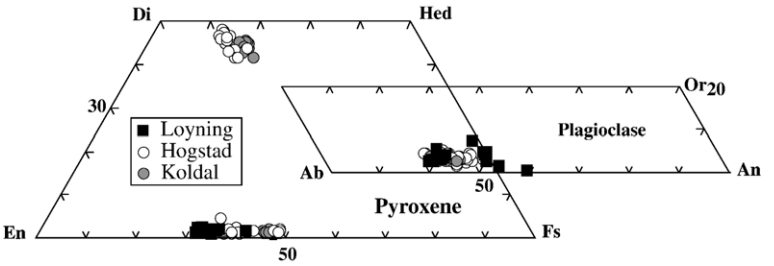

Fig. 5. Feldspar and pyroxene compositions. For Hogstad, each point represents the average of several analyses. For Løyning and Koldal, each point corresponds to one analysis.

dikes display significantly more enriched signatures with Sr_i ranging from 0.70564 to 0.70580 and ε_{Ndt}= −1.4 (GE30) (Table 9).

In Hogstad, cryptic layering is also restricted (Fig. 7). The An content of plagioclase is relatively constant in the banded norites, decreases in sample 6, increases in the mottled leuconorite (7) and then decreases towards the roof of the intrusion. Compositional changes shown by orthopyroxene are grossly parallel to those of plagioclase with, notably, a decrease in Mg# at the top of the banded norites. The slight differences in orthopyroxene's Mg# in samples 6, 7 and 9 are probably within analytical errors. Sr_i varies from 0.70537 to 0.70588 and ε_{Ndt} from +2.1 to −0.5. Sr_i variations are similar to variations in mineral compositions. Indeed, the strong decrease in Sr_i in sample 6, which has the lowest Sr_i (0.70537), is correlated with the decrease in plagioclase An content and in the orthopyroxene's Mg#. Moreover, the sharp increase in Sr_i at the base of the homogeneous gabbronorites is correlated with a decrease in plagioclase An content, but with no significant change in orthopyroxene's Mg#. Sample 8 from the mottled leuconorites displays the highest ε_{Ndt} (+2.1).

Compositional variations of minerals from the Koldal intrusion are shown as a function of the SiO_2 content of the whole rock on Fig. 8. Sr_i varies from 0.70680 to 0.70911, distinctly higher than in Løyning and Hogstad, and ε_{Ndt} from +3.5 to −1.6. The Sr_i of the apatite-bearing norites (samples 80-7-2 and 80-7-9: Sr_i=0.70803–0.70853) are higher than in the leuconorites lacking apatite (89-22 and 80-7-22: Sr_i=0.70709–

Table 3
Microprobe analyses of olivines

Løyning	GE-7	GE-8	GE-23
SiO_2	36.19	36.57	36.90
TiO_2	0.02	0.00	0.00
Al_2O_3	0.02	0.01	0.01
FeO	32.30	33.02	30.87
MnO	0.13	0.30	0.28
MgO	31.15	31.91	33.38
Total	99.81	101.81	101.44
Si	0.991	0.984	0.986
Al	0.001	0.000	0.000
Ti	0.000	0.000	0.000
Fe	0.739	0.743	0.690
Mn	0.003	0.007	0.006
Mg	1.271	1.280	1.329
∑Cations	3.005	3.014	3.011
Fo	63.1	63.1	65.6
Fa	36.7	36.6	34.1

Table 4
Trace element analyses (XRF, ppm) of magnetites, ilmenites and orthopyroxenes from Hogstad

Magnetites			
Sample	1	7	10
Ni	80	371	108
Co	84	84	<
Zn	370	1117	1117
Cr	1115	4419	452
Mn	155	155	620
V	5323	5499	5180

Ilmenites				
Sample	1	6	7	10
Ni	110	72	102	39
Co	242	190	209	51
Zn	–	–	–	–
Cr	178	<	486	59
Mn	2556	3020	2323	2865
V	1476	1704	1571	388

Orthopyroxenes				
Sample	1	6	7	10
Ni	155	88	92	40
Co	149	149	138	148
Zn	408	345	383	345
Cr	<	<	25	<
Mn	2865	2711	3098	3253
V	83	89	76	72

<: below detection limits, –: not determined.

Table 5
Trace elements content of apatites from Hogstad (ICPMS, ppm)

Sample	1	4	5	6	7	9	10	13	D[a]
La	312	218	275	352	328	543	385	823	4.6
Ce	1248	954	885	1155	1048	1761	1068	1620	5.7
Pr	154	81	151	188	173	286	165	248	6.7
Nd	1100	792	775	946	887	1412	824	1229	7.8
Sm	262	168	179	218	208	322	183	274	9.9
Eu	17	16	17	20	18	24	22	26	7.0
Gd	242	179	191	210	199	312	174	173	8.6
Tb	32	24	25	28	26	41	22	22	8.0
Dy	161	119	120	139	135	208	112	113	7.3
Ho	27	20	20	23	23	35	19	19	6.5
Er	67	50	46	57	57	89	47	49	5.7
Tm	6.9	5.2	4.4	5.9	6.1	9.3	4.9	5.2	5.0
Yb	35	26	21	30	31	47	25	28	4.2
Lu	4.2	3.2	2.5	3.6	3.7	5.7	3.1	3.5	3.4
Sr	342	306	362	333	357	406	414	697	

[a] REE partition coefficients between apatite and melt (Watson and Green, 1981).

0.70797). Samples 89-25 and 89-26 from the dike outcropping close to the roof of the intrusion have similar Sr_i (0.70773–0.70782) to those measured in Koldal.

Magnetites, ilmenites and orthopyroxenes separated from samples from the Hogstad intrusion have been analyzed for transition elements (V, Cr, Mn, Co, Ni, Zn: Table 4). As could be suspected from partition coefficient data, magnetites have higher contents of V and Cr and lower contents of Mn than ilmenites and orthopyroxenes. Magnetite from sample 7 (mottled leuconorite) has the highest contents in Cr, V and Ni, which correlate with the highest An content of its plagioclase (see Fig. 7).

Table 6
Trace element content of whole-rock samples from Løyning (ICPMS, ppm)

Sample	GE-6	GE-8	GE-9	GE-11	GE-12	GE-13	GE-19
Rb	0.9	1.8	2.6	1.1	3.4	3.3	3.6
Sr	400	196	392	202	961	9.7	816
Ba	126	56	144	47	211	16.6	195
Ga	16	9	12	15	24	13	16
Zr	38	44	10	20	11	55	<
Pb	2.7	2.1	<	2.1	2.8	<	35
Y	3.3	4.6	3.1	3.7	1.1	7.0	1.2
La	23	0.96	1.0	2.3	2.2	0.91	1.8
Ce	2.6	1.4	1.8	2.8	3.7	2.1	3.1
Pr	0.33	0.27	0.26	0.35	0.49	0.33	0.43
Nd	1.6	1.4	1.1	1.7	2.1	1.7	1.5
Sm	0.38	0.49	0.32	0.51	0.28	0.66	0.30
Eu	0.55	0.46	0.58	0.29	0.84	0.14	0.82
Gd	0.45	0.65	0.33	0.65	0.29	0.87	0.26
Tb	<	0.11	0.07	<	<	<	0.04
Dy	0.42	0.78	0.49	0.64	0.18	0.92	<
Ho	0.10	0.16	0.09	0.16	<	0.24	0.04
Er	0.21	0.44	0.27	0.40	0.11	0.59	0.12
Tm	0.03	0.08	0.06	0.06	0.01	0.09	0.02
Yb	0.22	0.52	0.33	0.40	0.08	0.60	0.10
Lu	0.03	0.06	0.05	0.06	0.01	0.10	0.02

<: below quantification limit.

REE patterns of whole-rock samples from the three intrusions are shown on Fig. 9. Most patterns display strong positive Eu anomalies reflecting plagioclase accumulation. Nevertheless, sample 10 from Hogstad and samples 80.7.9 and 89-23 from Koldal have higher bulk REE contents and either no Eu anomaly or a small positive one. In these samples, abundant cumulus apatite with strong negative Eu anomalies (Watson and Green, 1981) has swamped the positive Eu anomaly produced by plagioclase.

4.3. Discussion

Compositional and isotopic variations with stratigraphic height indicate that despite their restricted volumes, the mafic intrusions studied here have experienced open differentiation. In Løyning (Fig. 6), the transition between the Lower and Upper Units is underlined by an abrupt decrease in plagioclase An content correlated with a significant increase in ε_{Ndt} from 2.7 to 6.2. A possible explanation is that the Upper Unit crystallized from a new influx of magma with a lower An content, a higher ε_{Ndt} and similar Mg# and Sr_i than the parent magma of the Lower Unit. Indeed, assimilation of more enriched material is not supported by available isotopic data on the surrounding migmatitic gneisses, which have Sr_i above 0.707 and negative ε_{Ndt} (Bolle et al., 2003; Vander Auwera et al., 2003). Similarly in Hogstad (Fig. 7), the mottled leuconorites have several geochemical characteristics pointing to a

Table 7
Major (XRF, wt.%) and trace elements (ICP-MS, ppm) analyses of whole rocks from Hogstad

Sample	1	5	6	9	10	8
SiO_2	50.46	40.87	51.15	50.02	41.38	47.31
TiO_2	2.80	8.01	1.59	3.84	6.45	4.15
Al_2O_3	21.54	11.35	16.14	17.06	12.95	20.91
FeOt	8.41	22.21	10.23	11.36	18.81	8.55
MnO	0.18	0.16	0.20	0.10	0.09	0.19
MgO	2.67	8.46	7.94	6.09	7.15	3.06
CaO	8.22	4.55	6.91	7.40	7.35	8.23
Na_2O	4.15	1.35	3.00	2.33	1.80	5.02
K_2O	0.78	0.31	0.64	0.69	0.50	0.71
P_2O_5	0.10	0.09	0.40	0.39	1.61	0.35
LOI	0.33		0.13			0.10
Total	99.64	97.36	98.33	99.28	98.09	98.58
Rb	11	6.5	9.6	8.2	8.8	4.2
Sr	801	438	608	623	486	719
Ba	332	182	335	334	280	325
Ga	25	22	20	20	22	22
Zr	72	87	72	140	111	86
Nb	6.0	14	5.2	9.9	13	5.3
Ta	0.45	0.87	0.60	0.73	1.0	0.53
Pb	7.4	6.6	17	4.1	2.3	5.2
Y	7.9	6.9	22	23	40	13
La	6.9	3.2	13	19	23	10
Ce	14	5.1	30	34	52	22
Pr	1.5	0.4	4.0	4.5	7.7	3.2
Nd	5.6	1.5	19	20	39	15
Sm	1.1	<	4.1	4.4	9.0	3.1
Eu	1.6	0.81	2.0	1.9	3.0	1.7
Gd	<	<	3.8	4.4	8.6	3.3
Tb	<	<	0.61	0.69	1.3	<
Dy	0.69	0.33	3.1	3.2	6.3	2.4
Ho	<	<	0.62	0.70	1.2	0.48
Er	0.56	0.50	1.7	2.0	3.2	1.1
Tm	<	<	0.22	0.23	0.37	0.14
Yb	<	<	1.1	1.3	1.9	0.94
Lu	<	<	0.18	0.20	0.28	0.14

<: below quantification limit. Major elements as wt.% oxide and trace elements.

new influx of magma. In sample 7, plagioclase has a slightly higher An content (An_{46}) and Fe–Ti oxides (ilmenite, magnetite) display the highest V, Cr and Ni contents. Samples from the mottled leuconorites also have low Sr_i (0.70543–0.70545) and the highest ε_{Ndt} (+2.1). Sample 6 located at the upper limit of the banded norites unit is characterized by a well-defined modal layering and has thus been included in this unit. Nevertheless, compared with the other samples from the same unit, it has a significantly lower Sr_i. This suggests that this ratio might have been influenced by the new influx of magma and/or a faster Sr isotopic (self) diffusion than elemental (chemical) diffusion (Baker, 1990).

Some degree of assimilation of more enriched material during differentiation may be responsible for some irregular variations of Sr_i and ε_{Ndt} along stratigraphic height. Sr_i increases in the banded and homogeneous gabbronorites from Hogstad and ε_{Ndt} from the two analyzed samples from the Lower Unit of Løyning are strongly different. These observations are nevertheless paradoxical as these intrusions were emplaced in anorthosite having lower Rb/Sr ratios than the supposed jotunitic parent magmas (see Section 5). Also, Sr isotopic data from the Tellnes dike outcropping in the middle of the Åna-Sira anorthosite have revealed that it evolved by fractional crystallization without any contamination (Wilmart et al., 1989). Possibly, some assimilation of the surrounding migmatitic gneisses might have occurred as the intrusions were emplaced close to the contacts. It is also plausible that the small magma chambers result from the collection of

Table 8
Major (XRF, wt.%) and trace element (ppm) data for whole-rock samples from Koldal

Sample	80.7.9	80.7.26	89.22	89.23	89.27	90.26
SiO_2	45.18	58.29	56.49	49.56	59.92	58.52
TiO_2	5.36	1.00	0.88	3.57	0.91	1.32
Al_2O_3	14.72	18.77	22.16	16.11	18.88	19.46
FeOt	15.36	5.95	3.87	9.62	4.70	4.60
MnO	0.14	0.09	0.05	0.12	0.06	0.08
MgO	4.72	1.63	1.76	4.38	1.28	1.89
CaO	8.27	4.30	7.71	8.85	3.26	4.94
Na_2O	3.66	4.98	5.23	3.82	4.79	4.97
K_2O	0.37	4.38	0.79	1.10	5.08	3.53
P_2O_5	1.45	0.10	0.26	1.82	0.09	0.34
Total	99.84	99.79	99.63	100.02	99.49	100.16
Rb	<	13	<	<	19	5.6
Sr	413	460	794	559	446	550
Ba	193	2357	818	661	2374	2238
Ga	24	27	33	25	26	25
V	369	37	43	254	66	28
Co	32		13	44	12	<
Zn	111	63	33	63	32	28
Zr	27	20	<	15	14	<
Nb	5.3	<	<	1.8	<	<
Y	15	1.4	3.2	21	0.30	2.6
La	4.80	1.66	2.08	6.95	0.88	1.17
Ce	13.2	3.45	3.91	17.6	1.84	2.33
Pr	2.32	0.44	0.53	3.09	0.21	0.36
Nd	13.0	2.21	2.66	17.8	1.01	2.60
Sm	3.40	0.38	0.55	4.53	0.18	0.91
Eu	1.61	3.73	2.00	2.43	3.88	4.41
Gd	3.84	0.62	0.59	5.43	0.30	1.17
Dy	2.58	0.26	0.46	3.40	0.15	0.52
Ho	0.55	0.06	0.12	0.67	0.04	0.10
Er	1.17	0.13	0.20	1.38	0.08	0.17
Tm	0.13	0.01	0.03	1.61	0.01	0.02
Yb	0.77	0.10	0.12	0.83	0.06	0.10
Lu	0.12	0.01	0.01	0.12	0.01	0.01

XRF: Ba (except 80.7.26: ICPMS), V, Co, Zn.
ICPMS: REE, Y, Rb, Sr (except for sample 89-22:XRF), Ga, Zr, Nb.

Table 9
Sr and Nd isotopic compositions in plagioclase separates (pl) or whole-rock (wr) samples from Løyning, Hogstad and Koldal

Samples		Description	Rb (ppm)	Sr (ppm)	$^{87}Sr/^{86}Sr$	2σ	Nd (ppm)	Sm (ppm)	$^{87}Rb/^{86}Sr$	Sr_i at 930 Ma	$^{147}Sm/^{144}Nd$	$^{143}Nd/^{144}Nd$	2σ	$^{143}Nd/^{144}Nd$ at 930	ε_{Nd} at 930
Løyning															
GE-6	wr	Norite	0.9	400	0.704404[a]	6	1.6	0.38	0.007	0.70432	0.1413	0.512602	12	0.51174	5.9
GE-8	wr	Olivine-bearing melanorite	1.8	196	0.704243	7	1.4	0.50	0.026	0.70389					
GE-9	wr	Norite	2.6	392	0.704822	7	1.1	0.30	0.019	0.70457					
GE-11	wr	Melanorite	1.1	202	0.704079[a]	9	1.7	0.51	0.016	0.70387	0.1852	0.512707[a]	14	0.51158	2.7
GE-12	wr	Leuconorite	3.4	961	0.703988[a]	10	2.1	0.28	0.010	0.70385	0.0816	0.512254	9	0.51176	6.2
GE-19	wr	Leuconorite	3.6	816	0.703929	7	1.5	0.30	0.013	0.70376					
GE-20	wr	Anorthositic dike	9.0	713	0.706278	6	2.5	0.50	0.037	0.70579					
GE-31	wr	Leuconoritic dike	7.0	547	0.706289	9	<0.5	0.16	0.037	0.70580					
GE-30	wr	Leuconoritic dike	2.8	580	0.70583[a]	8	1.5	0.35	0.014	0.70564	0.1466	0.512259	13	0.51136	−1.4
Hogstad															
14	pl	Banded norite	6.1	928	0.705879[a]	8	5.2	0.72	0.019	0.70563	0.0841	0.511923	7	0.51141	−0.5
4	pl	Banded norite	4.4	903	0.70588[a]	7	5.1	0.61	0.014	0.70569	0.0716	0.511955	10	0.51152	1.6
1	pl	Banded norite	1.8	890	0.705804	7	3.2	0.54	0.006	0.70573					
2	pl	Banded norite	2.3	998	0.705775	7	5.1	0.71	0.007	0.70569					
5	pl	Banded norite	0.4	912	0.705861	8	3.2	0.43	0.001	0.70584					
7	pl	Leuconorite	2.1	916	0.705516	8	3.3	0.79	0.007	0.70543					
9	pl	Homogeneous gabbronorite	2.7	815	0.705801	26	4.2	0.60	0.010	0.70567					
10	pl	Homogeneous gabbronorite	1.1	923	0.705748	7	2.3	0.46	0.004	0.70570					
6	pl	Banded norite	1.9	917	0.705453	7	4.2	0.81	0.006	0.70537					
13	pl	Homogeneous gabbronorite	4.9	885	0.706096	7	5.9	0.93	0.016	0.70588					
8	wr	Mottled leuconorite	4.2	719	0.705671[a]	6	15	3.1	0.017	0.70545	0.1295	0.512333	10	0.51154	2.1
Koldal															
80.7.2	pl	Leuconorite	4.6	923	0.708224	39	1.3	0.15	0.014	0.70803					
80.7.9	wr	Leuconorite	0.4	413	0.708568[a]	6	13	3.4	0.003	0.70853	0.1585	0.51241	9	0.51144	0.1
80.7.22	pl	Leuconorite	1.6	750	0.708054	7	0.7	0.05	0.006	0.70797					
80.7.23	pl	Leuconorite	3.3	821	0.706193	8	2.6	0.36	0.012	0.70604					
80.7.26	wr	Mangerite	13	460	0.710231[a]	6	2.2	0.38	0.084	0.70911	0.1043	0.512253	8	0.51162	3.5
89.22	wr	Leuconorite	0.6	794	0.707123[a]	8	2.7	0.55	0.002	0.70709	0.1245	0.512295	13	0.51154	1.9
89.25	wr	Jotunite	13	463	0.708904	6	99	22	0.081	0.70782					
89.26	wr	Jotunite	13	465	0.708803	7	79	19	0.081	0.70773					
89.27	wr	Mangerite	19	446	0.709471[a]	6	1.0	0.18	0.122	0.70784	0.1052	0.512015	58	0.51137	−1.3
90.26	wr	Mangerite	6	550	0.707529[a]	6	2.6	0.91	0.029	0.70714	0.2114	0.512644	13	0.51135	−1.6
90.32	wr	Mangerite	17	424	0.708345	9	<	0.89	0.116	0.70680					
89.23	wr	Jotunite	0.7	559	0.706636	5	18	4.5	0.004	0.70659	0.1539	0.512446[a]	5	0.51151	1.4

ICPMS data for Rb, Sr, Nd and Sm except in 89.22 (XRF).
[a] Average of duplicates (see text).

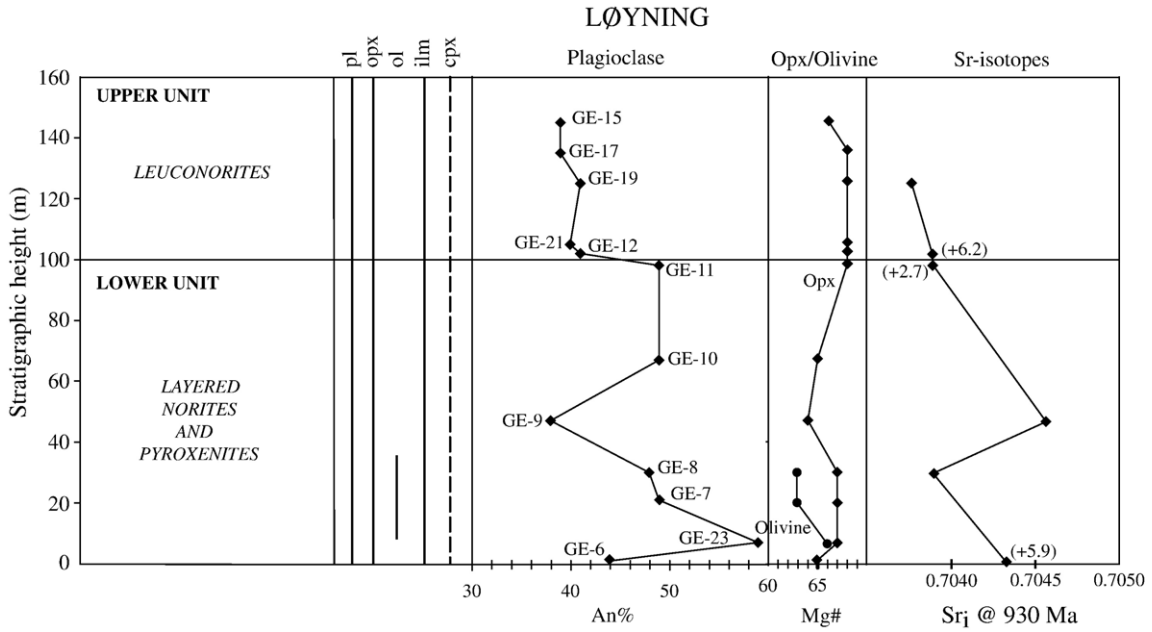

Fig. 6. Generalized cumulus sequence and cryptic layering in the Løyning body. Dashed line: intercumulus phase, continuous line: cumulus phase. Abbreviations: pl=plagioclase, opx=orthopyroxene, ol=olivine, ilm=ilmenite, cpx=clinopyroxene. Selected plagioclase and pyroxene compositions are close to the average composition observed in each sample. Olivine compositions are given as forsterite content. ε_{Ndt} are given in brackets.

magma batches with variable isotopic compositions, which would have migrated through the anorthositic crystal mush. This hypothesis will be further discussed in Section 7.

The least differentiated compositions of plagioclase and orthopyroxene observed in the three intrusions suggest that the parent magmas were progressively more differentiated in the sequence Løyning–Hogstad–

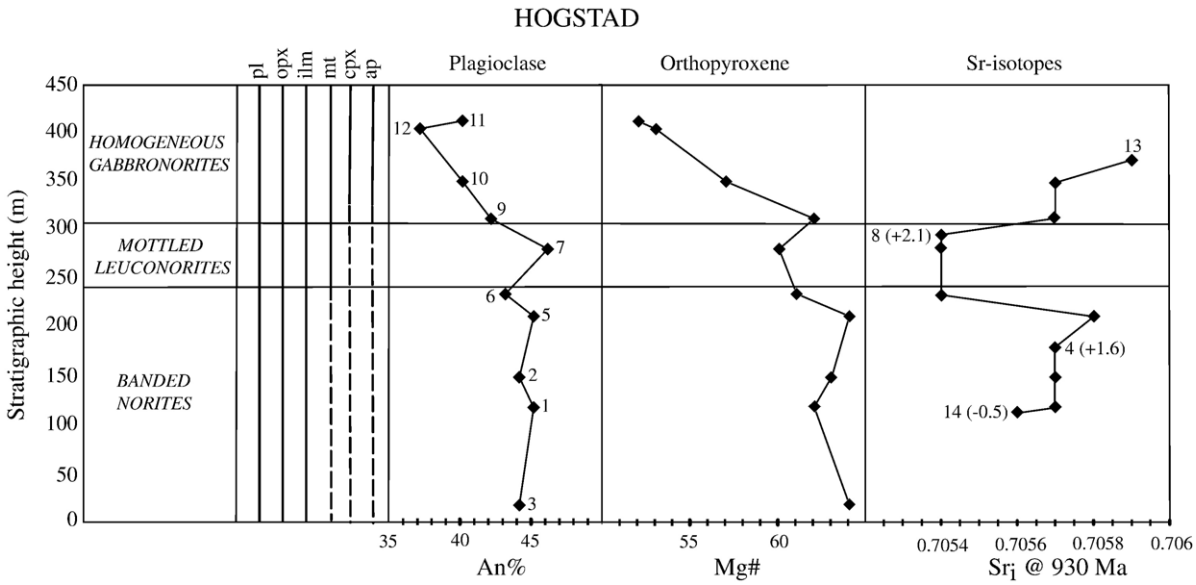

Fig. 7. Generalized cumulus sequence and cryptic layering in the Hogstad body. Dashed line: intercumulus phase, continuous line: cumulus phase. Abbreviations: pl=plagioclase, opx=orthopyroxene, ilm=ilmenite, mt=magnetite, cpx=clinopyroxene, ap=apatite. Plagioclase and pyroxene compositions are averages of several microprobe analyses. ε_{Ndt} are given in brackets.

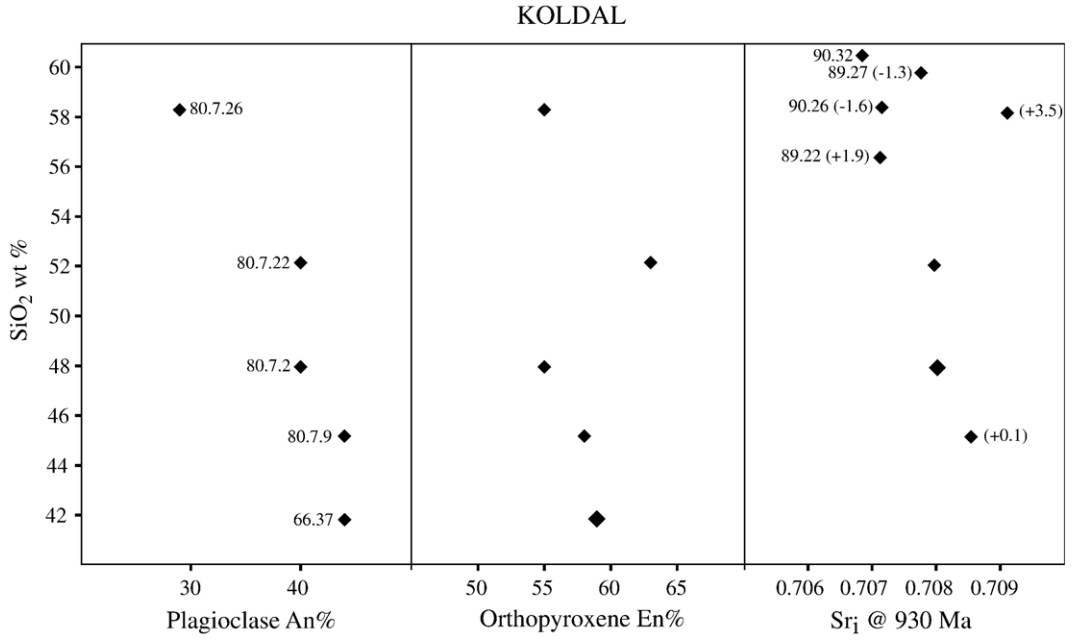

Fig. 8. Mineral compositions (corresponding to single analyses) and $^{87}Sr/^{86}Sr$ ratios (at 930 Ma) versus SiO_2 (wt.%) in the Koldal body. ε_{Ndt} values (at 930 Ma) are given in brackets.

Koldal with a stronger effect on plagioclase composition: An_{59}–En_{68} in Løyning, An_{49}–En_{64} in Hogstad and An_{44}–En_{61} in Koldal. Isotopic data also indicate that parent magmas had progressively more enriched signatures as the Sr_i ranges are 0.70376 to 0.70457 in Løyning, 0.70537 to 0.70588 in Hogstad and 0.70659 to 0.70911 in Koldal. Also, the highest ε_{Ndt} (+6.8) was measured in Løyning and the lowest (−1.6) in Koldal.

5. Parent magmas of the marginal mafic intrusions

As previously discussed, we admit that the layering developed horizontally and then tilted into subvertical position during the late movements of the anorthositic diapirs. Accordingly, the parent magmas of these intrusions were emplaced in the diapirs before its final movements. Also, mineral parageneses observed in the three mafic intrusions are similar to those of the Bjerkreim-Sokndal layered intrusion for which a parent magma more magnesian and anorthitic than the TJ primitive jotunite has been inferred (Vander Auwera and Longhi, 1994). The parent magmas of the mafic intrusions thus most probably belong to the jotunite kindred. This suggests a possible genetic link between the enclosing anorthosites and the parent magmas of the mafic intrusions. The orthopyroxene and plagioclase megacrysts from the enclosing anorthosites have slightly less differentiated compositions ($En_{75–74}$, $An_{55–49}$) (Duchesne and Maquil, 2001) than in the small intrusions ($En_{68–61}$, $An_{59–44}$) with a greater difference in the orthopyroxene's Mg#. Moreover, Sr and Nd isotopic compositions of the mafic intrusions partly overlap the observed range in the anorthosites: Sr_i=0.7033 to 0.7063, ε_{Nd}=+5.9 to −1.8 (Demaiffe et al., 1986). It thus seems that the parent magmas of the mafic intrusions were slightly more differentiated (lower Mg# and An%) than those of the enclosing anorthosites and are thus probably residual after anorthosite fractionation. The least differentiated compositions of plagioclases and orthopyroxenes (Løyning: Ens_{68}–An_{59}, Hogstad: Ens_{64}–An_{49}, Koldal: Ens_{61}–An_{44}) are similar to those that crystallized in experiments on the TJ primitive jotunite (Ens_{66}–An_{47}: Vander Auwera and Longhi, 1994) and 75202F, an evolved jotunite (Fo_{50}–An_{43}: Vander Auwera et al., 1998a). This suggests that the parent magma of Løyning was more anorthitic and slightly more magnesian than the TJ primitive jotunite, the parent magma of Hogstad was very similar to TJ, and that of Koldal, to an evolved jotunite.

As already exposed in the introduction, the jotunite suite of Rogaland has been interpreted as a result of multi-stage fractional crystallization (Vander Auwera et al., 1998a). In the early stage, a primitive jotunite (high Mg#, low K_2O) differentiated to an evolved jotunite by subtraction of a leuconoritic cumulate composed of 70% plagioclase, 20% orthopyroxene and 10% ilmenite

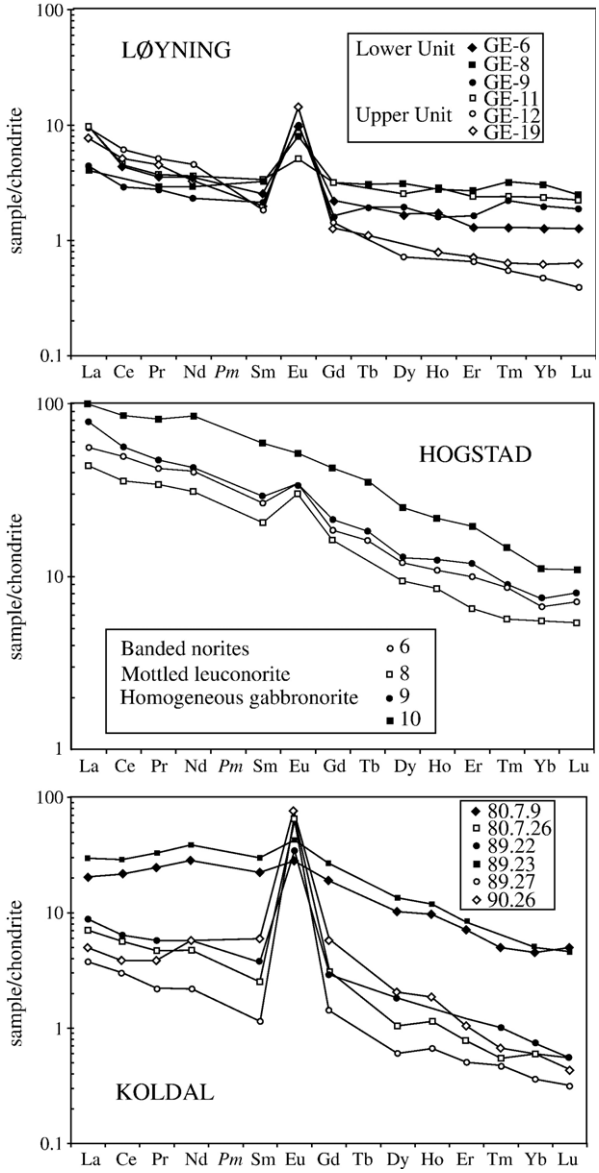

Fig. 9. REE contents of whole-rock samples from Løyning, Hogstad and Koldal. Chondrite values are from Sun and McDonough (1989).

(Duchesne, 1978; Vander Auwera et al., 1998a). In the second stage, evolved jotunite differentiated to a mangerite by subtraction of a noritic cumulate (43% plag+20% opx+9% cpx+9% ilm+11% mgt+8% apatite) and the final stage involves differentiation from a mangerite to a quartz mangerite by subtraction of a gabbronoritic cumulate (47% plag+11% opx+13% cpx+3% ilm+21% mgt+5% apatite) (Duchesne, 1978; Wilmart et al., 1989; Vander Auwera et al., 1998a). Moreover, it has been shown that the parent magmas of the andesine anorthosites are slightly more magnesian and more anorthitic than the TJ primitive jotunite studied by Vander Auwera and Longhi (1994). This parent magma is thus supposed to have differentiated in a lower crustal magma chamber (10–13 kbar) to produce anorthositic and leuconoritic cumulates as well as collected residual melts broadly jotunitic in composition. As the plagioclase-rich accumulations were sufficiently buoyant, an anorthositic diapir containing a certain amount of residual melts, possibly the parent magmas of the mafic intrusions, was formed and rose through the crust.

Trace element content of cumulus minerals can be used to evaluate the trace element composition of parent

magmas if the following conditions are fulfilled: minerals must have equilibrated with the melt; partition coefficients should be appropriate for the melt and mineral compositions as well as for the temperature of equilibrium; minerals must have retained their equilibrium composition, i.e. subsolidus reequilibration and reaction with trapped melt should be minimal. In this study, we have considered the REE contents of apatite in the Hogstad body for the following reasons. Apatite is present throughout the Hogstad body, as an intercumulus phase in the lower part and as a cumulus phase in the upper part, and the stratigraphy of this intrusion is well constrained. REE partition coefficients between apatite and liquid have been experimentally measured (Watson and Green, 1981) (Table 5). REE being strongly compatible in apatite, the REE content is very high, thus decreasing analytical uncertainties and minimizing the effect of the possible presence of inclusions. Moreover, the effect of reequilibration with trapped melt, the "trapped liquid shift effect" of Barnes (1986), can be ignored (Cawthorn, 1996). Finally, the possibility that the REE composition of apatite could have been modified during subsolidus cooling should be addressed. Indeed, during the slow cooling of layered intrusions, diffusion could significantly modify the distribution of trace elements within and among minerals. Diffusive reequilibration of REE between apatite and coexisting minerals during subsolidus cooling could have occurred, the driving force being chemical disequilibrium between phases. In this case, this chemical disequilibrium could appear in response to decreasing temperature and corresponding changes in the equilibrium partition coefficients. This hypothesis can be tested using the new diffusion coefficients and closure temperatures of REE in apatite estimated by Cherniak (2000) and data from the modelling of the thermal aureole induced by the emplacement of the Rogaland Anorthositic Province (Westphal et al., 2003). Using 2D thermal modelling, these authors have shown that, at around 500 m from the intrusions, the average cooling rate between 1050 °C and 800 °C was 60 °C/Ma. Using new REE diffusion coefficients in apatite, Cherniak (2000) estimated the closure temperatures with the formalism of Dodson (1973) as a function of the effective diffusion radius and for a cooling rate of 10 °C/Ma. For an average grain size of 3 mm, closure temperatures of apatite for Nd is 920 °C. This is a minimum estimate as a cooling rate higher than 10 °C/Ma will increase closure temperatures. The very high closure temperatures estimated for apatite suggest that subsolidus redistribution of REE in the Hogstad intrusion was minor. The REE content of liquids in equilibrium with apatite from the three units of Hogstad are displayed on Fig. 10 and compared with REE patterns of primitive and evolved jotunites. These calculated REE contents are in the range of those

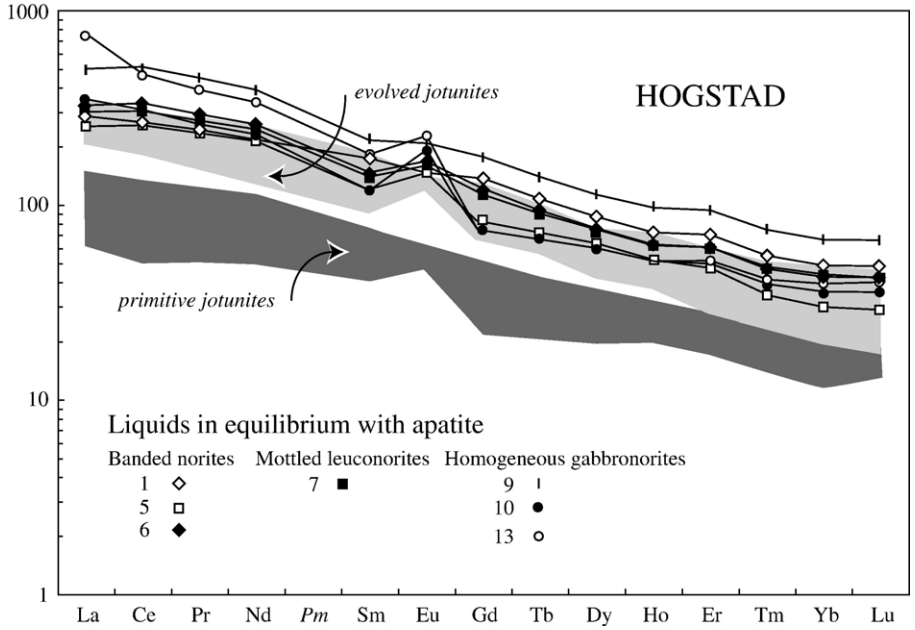

Fig. 10. Calculated REE contents of melts in equilibrium with intercumulus (banded norites, mottled leuconorites) and cumulus (homogeneous gabbronorites) apatite from Hogstad using partition coefficients of Watson and Green (1981) (Table 5) (see text for explanation). Data for primitive and evolved jotunites are from Vander Auwera et al. (1998a).

measured on evolved jotunites. Also, liquids calculated from cumulus and intercumulus apatite display similar REE patterns with only a higher total REE content for liquid 9 and a slightly higher LREE fractionation for liquid 13. This suggests that the intercumulus liquid present in the banded norites and mottled leuconorites was similar to the melt in equilibrium with the homogeneous gabbronorites. Major and trace elements thus indicate that, in Hogstad, the melt in equilibrium with the banded norites and mottled leuconorites was a primitive jotunite and the intercumulus liquid, an evolved jotunite when it started crystallizing intercumulus apatite. In the homogeneous gabbronorites, the melt had the composition of an evolved jotunite.

In conclusion, major element compositions of plagioclase and orthopyroxene together with calculated REE patterns of liquids in equilibrium with cumulus and intercumulus apatites from the Hogstad intrusion indicate that the parent magma of Løyning was more anorthitic and slightly more magnesian than the TJ primitive jotunite; the parent magma of Hogstad was a primitive jotunite and that of Koldal, close to an evolved jotunite. The good match between the Sr and Nd isotopic compositions observed in the three intrusions and those reported for primitive and evolved jotunites (Bolle et al., 2003) further support this conclusion.

6. Density calculations

As the molar volumes of natural silicate melts can be expressed as linear function of composition, temperature and pressure, silicate melt densities can readily be calculated using model equations (Lange and Carmichael, 1990; Vander Auwera and Longhi, 1994; Scoates, 2000).

The calculated densities of primitive and evolved jotunites strongly depend on their Fe^{3+}/Fe^{2+} ratios as well as their P_2O_5 (Toplis et al., 1994) and volatile contents (Lange, 1994). Experimental data acquired on these liquids (Vander Auwera and Longhi, 1994; Vander Auwera et al., 1998a) suggest oxygen fugacities close to FMQ during crystallization and liquidus temperatures around 1150 °C for the primitive jotunites and 1135 °C, for the evolved jotunites. Using the regression of Kress and Carmichael (1991) which incorporates the effects of composition, temperature, oxygen fugacity and pressure on the redox state of the magma, the Fe^{3+}/Fe^{2+} ratios of primitive and evolved jotunites have been calculated. Pressure estimates for the final emplacement of the Egersund-Ogna and Åna-Sira massif anorthosites range between 3 and 5 kb and are based on experimental data (Vander Auwera and Longhi, 1994) and M2 contact metamorphic phase equilibria (Jansen et al., 1985; Holland et al., 1996). A conservative value of 3 kb has been considered in the calculation. Under these conditions, the average Fe_2O_3/FeO is 0.16 for primitive and evolved jotunites.

Volatile components such as H_2O, CO_2 and F usually make up a small proportion of magmas associated with massif-type anorthosites. Indeed, mineral parageneses observed in the contact aureoles of anorthosites complexes and in the massif-type anorthosites themselves indicate a very low a_{H2O} (Morse, 1982; Fuhrman et al., 1988; Kolker and Lindsley, 1989). Nevertheless, because of their low molecular weights, these very low concentrations may translate into significant mole fractions. The effect of these volatile components on melt density should thus quantitatively be assessed even if probably negligible (Lange, 1994; Scoates, 2000).

In order to incorporate the effect of volatiles in the density calculation, volatiles contents of jotunites have been estimated in the following way. An H_2O content of 0.15% has been selected as experiments performed on a high-Al basalt containing less than 0.15% H_2O successfully reproduced the mineral parageneses observed in the Harp Lake complex (Fram and Longhi, 1992). The measured F content of the TJ primitive jotunite is 435 ppm (I. Roelandts, pers. comm.). All other parameters being constant, doubling the F or H_2O contents reduces the calculated densities by 0.0006 g/cm^3 and 0.007 g/cm^3, respectively. The CO_2 content of primitive jotunites is uncertain. We have used a value of 200 ppm in the following discussion based on data acquired on submarine MORB glasses (Johnson et al., 1994; Scoates, 2000). Nevertheless, it turns out that the effect of CO_2 is also small as the calculated density of the primitive jotunite is 2.733 for 200 ppm CO_2 and 2.732 for 1000 ppm CO_2. Using the model of fractional crystallization of Vander Auwera et al. (1998a), the volatile content of the evolved jotunites has been calculated to 870 ppm F, 0.30% H_2O and 400 ppm CO_2. Uncertainties as to the values of partial molar volumes of CO_2, H_2O and F in natural silicate melts are significant and values proposed by Lange (1994) have been considered here. Results are shown in Fig. 11 and compared with the density of plagioclase (Campbell et al., 1978). Plausible parent magmas of the mafic intrusions are clearly denser than the plagioclase of an anorthositic crystal mush.

7. Discussion

The major and trace element compositions of the three mafic intrusions indicate parent magmas with

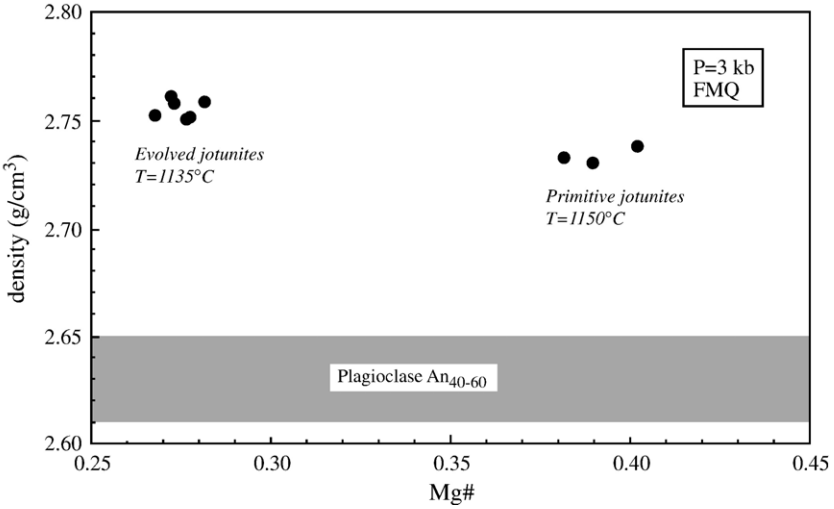

Fig. 11. Calculated densities versus Mg# for primitive and evolved jotunites (see text for explanation) compared to the density of plagioclase (Campbell et al., 1978).

broadly jotunitic compositions, i.e. in the compositional range of melts residual to massif-type anorthosite formation. Given also that these small magma chambers were included in the margins of the anorthosites before the final movements of the diapirs, it is plausible that they represent residual melts which were entrained within the anorthositic diapir up to its final level of emplacement. The presence of a certain amount of liquid is indeed required to enable the transport of the diapir through the crust (e.g. Longhi et al., 1993). Field and geochemical evidence suggest that, in the Rogaland Province, residual melts after anorthosite formation were collected into two different ways. Part of these residual liquids was collected in magma chambers, which finally produced small layered intrusions having a subvertical layering concordant with the foliation of the surrounding anorthosite (Løyning, Hogstad). The rest of these liquids was emplaced as dikes crosscutting the anorthosites (i.e. Hadland, Lomland, Varberg: Fig. 1) (Vander Auwera et al., 1998a). The Koldal intrusion appears intermediate between these two settings as its northern part crosscuts the enclosing anorthosite, whereas in its southern part the subvertical layering is concordant with the foliation of the anorthosite. It is worth noting that the parent magmas of Løyning and Hogstad are less differentiated (Løyning: more anorthitic and more magnesian than a primitive jotunite; Hogstad: primitive jotunite) than the parent magmas of the Koldal intrusion (evolved jotunite) and of the dikes (evolved jotunites). The former ones are thus earlier in the differentiation and final consolidation of the anorthositic diapir than the latter ones.

We will now further examine possible ways of collecting residual melts in the anorthositic diapir in order to produce the small magma chambers of Løyning and Hogstad. The size of these intrusions is very limited compared to the extension of the enclosing anorthosites as they represent less than 0.5% of the exposed surfaces of these anorthosites. They formed rather early in the evolution of the diapir as shown by their parent magmas composition and by the fact that their layering was supposedly acquired horizontally and then tilted during the final movements of the diapir. The Løyning and Hogstad intrusions are restricted to the margins of the anorthosite and we have shown above that there was a strong density contrast between the plagioclase framework and the melt. If these dense residual melts are enclosed within an impermeable crystalline network, they will not be extracted and, upon crystallization, will produce leuconoritic to ferrodioritic rocks. If permeability is still present, dense residual melts could infiltrate downward and produce pods or dyklets of jotunitic (ferrodioritic) composition, which are characteristically observed in Proterozoic anorthosites (e.g. Vander Auwera and Duchesne, 1990). These two processes will however produce restricted masses of jotunitic composition. In order to produce the small magma chambers of Hogstad and Løyning, another process must be found. Efficient migration and draining of dense residual melt through the crystal mush could occur along a sloping floor as suggested by Morse (1986) and Scoates (2000). Emplacement of the anorthositic crystal mush as a rising diapir results in a domical structure with inclined floor along its margins, the floor being a more consolidated zone with lesser

permeability. This domical structure is consistent with the observed shape of Proterozoic anorthosites (e.g. Emslie, 1980). This process takes into account the restricted occurrence of the mafic intrusions in the margins of the massif anorthosites. However, it is also possible that the parent magmas of the Løyning and Hogstad intrusions were collected in small shear zones developed in the semi-consolidated crystal mush. Nevertheless, as mentioned above, the parent magmas of Løyning and Hogstad were collected in a rather early stage of the evolution of the diapir and this process was probably more likely in a later stage as discussed below.

In a later stage, when the anorthosite was nearly consolidated, the residual melts were more differentiated (evolved jotunites) and could have been filter pressed into extensional fractures generated in the cooling and contracting anorthositic body in a similar way as aplitic dikes emplace in granitic plutons (Hibbard and Watters, 1985) or into nearby small shear zones. With a small percentage of interstitial residual melt, the crystal rich mush will indeed fracture and behave in a brittle manner. The geological map of the Rogaland anorthositic complex clearly shows that these dikes are much more abundant than the small mafic intrusions. Collection and transport along dikes was thus probably more efficient than draining through the crystal mush.

The new influxes of magma evidenced by changes in isotopic and mineral compositions in the Løyning and Hogstad intrusions as well as irregular variations of Sr_i and ε_{Ndt} with stratigraphic height could represent batches of residual melts with variable isotopic compositions, collected in the small magma chambers. The unsuitability of anorthosites as a source of contamination suggests that these batches of jotunitic melts acquired their variably enriched isotopic signature before emplacement of the anorthositic diapirs. This process most probably took place either at their lower crustal source (Longhi et al., 1999) or during ascent in magma conduits from the lower crust ($\approx$11 kb) to the final level of emplacement ($\approx$4 kb). Furthermore, replenishment with isotopically distinct magma batches within small mafic intrusions like Løyning or Hogstad suggests that the building-up of one particular massif-type anorthosite involves several replenishments of isotopically distinct magmas. A similar conclusion has also been reached by Scoates and Frost (1996) in the Laramie anorthosite complex.

Acknowledgements

We would like to thank G. Bologne and G. Delhaze for their help in sample preparation and chemical analyses. J. Wauthier supervised the microprobe analyses. Claude Maerschalk (ULB) and Bruno Kieffer (UBC) are greatly thanked for their help in the chemical separation for Sr and Nd isotopic analyses. We thank two anonymous reviewers for constructive reviews, which helped to strengthen the manuscript. This work was funded by the Belgian Fund for Joint Research.

References

Ashwal, L.D., 1982. Mineralogy of mafic and Fe–Ti oxide-rich differentiates of the Marcy anorthosite massif, Adirondacks, NY. Amererican Mineralogist 67, 14–27.

Ashwal, L.D., 1993. Anorthosites. Springer Verlag, Heidelberg. 422 pp.

Baker, D.R., 1990. Chemical interdiffusion of dacite and rhyolite: anhydrous measurements at 1 atm and 10 kbar, application of transition state theory, and diffusion in zoned magma chambers. Contributions to Mineralogy and Petrology 104, 407–423.

Barnes, S., 1986. The effect of trapped liquid crystallization on cumulus mineral compositions in layered intrusions. Contributions to Mineralogy and Petrology 93, 524–531.

Bingen, B., van Breemen, O., 1998. U–Pb monazite ages in amphibolite- to granulite facies orthogneisses reflect hydrous mineral breakdown reactions: Sveconorwegian Province of SW Norway. Contributions to Mineralogy and Petrology 132, 336–353.

Bingen, B., Demaiffe, D., Hertogen, J., Weis, D., Michot, J., 1993. K-rich calc-alkaline augen gneisses of Grenvillian age in SW Norway; mingling of mantle-derived and crustal components. Journal of Geology 101, 763–778.

Bolle, O., 1996. L'Apophyse du massif stratiforme de Bjerkreim-Sokndal (Rogaland, Norvège): une intrusion composite de la suite charnockitique. In: Demaiffe, D. (Ed.), Petrology and Geochemistry of Magmatic Suites of Rocks in the Continental and Oceanic Crusts. ULB-MRAC, Bruxelles, pp. 129–144.

Bolle, O., 1998. Mélanges magmatiques et tectonique gravitaire dans l'Apophyse de l'intrusion de Bjerkreim-Sokndal (Rogaland, Norvège): pétrologie, géochimie et fabrique magnétique. PhD Thesis, Université de Liège, Belgium.

Bolle, O., Diot, H., Duchesne, J.C., 2000. Magnetic fabric and deformation in charnockitic igneous rocks of the Bjerkreim-Sokndal layered intrusion (Rogaland, southwest Norway). Journal of Structural Geology 22, 647–667.

Bolle, O., Trindade, R.I.F., Bouchez, J.L., Duchesne, J.C., 2002. Imaging downward granitic magma transport in the Rogaland Igneous Complex. Terra Nova 14, 87–92.

Bolle, O., Demaiffe, D., Duchesne, J.C., 2003. Petrogenesis of jotunitic and acidic members of an AMC suite (Rogaland Anorthosite Province, SW Norway): a Sr and Nd isotopic assessment. Precambrian Research 124, 185–214.

Bologne, G., Duchesne, J.C., 1991. Analyse des roches silicatées par spectrométrie de fluorescence X: précision et exactitude. Belgian Geological Survey Professional Paper 249 (5), 1–11.

Boutefeu, A., 1973. La lentille noritique de Hogstad (Norvège méridionale). Etude géologique, pétrologique et géochimique. Master Thesis, Liège. 60 pp.

Campbell, I., Roeder, P., Dixon, J., 1978. Plagioclase buoyancy in basaltic liquids as determined with a centrifuge furnace. Contributions to Mineralogy and Petrology 67, 369–377.

Castellani, M., 1993. La lentille de Hogstad (Rogaland, Norvège méridionale). Master Thesis, Liège. 80 pp.

Cawthorn, R., 1996. Models for incompatible trace-element abundances in cumulus minerals and their application to plagioclase and pyroxenes in the Bushveld complex. Contributions to Mineralogy and Petrology 123, 109–115.

Chauvel, C., Blichert-Toft, J., 2001. A hafnium isotope and trace element perspective on melting of the depleted mantle. Earth and Planetary Science Letters 190 (3–4), 137–151.

Cherniak, D., 2000. Rare earth element diffusion in apatite. Geochimica et Cosmochimica Acta 64 (22), 3871–3885.

Demaiffe, D., 1972. Etude pétrologique de l'Apophyse Sud-Est du massif de Bjerkreim-Sokndal (Norvège méridionale). Annales de la Société Géologique de Belgique 95 (2), 255–269.

Demaiffe, D., Hertogen, J., 1981. Rare earth geochemistry and strontium isotopic composition of a massif-type anorthositic-charnockitic body: the Hidra massif (Rogaland, SW Norway). Geochimica et Cosmochimica Acta 45, 1545–1561.

Demaiffe, D., Duchesne, J., Michot, J., Pasteels, P., 1973. Le massif anorthosito-leuconoritique d'Hidra et son faciès de bordure. Comptes rendus de l'Académie des sciences. Paris 277, 17–20.

Demaiffe, D., Weis, D., Michot, J., Duchesne, J.C., 1986. Isotopic constraints on the genesis of the Roagaland anorthositic suite (southwest Norway). Chemical Geology 57, 167–179.

Dodson, M., 1973. Closure temperature in cooling geochronological and petrological systems. Contributions to Mineralogy and Petrology 40, 259–274.

Duchesne, J.C., 1978. Quantitative modeling of Sr, Ca, Rb and K in the Bjerkreim-Sokndal lopolith (SW Norway). Contributions to Mineralogy and Petrology 66, 175–184.

Duchesne, J.C., Demaiffe, D., 1978. Trace elements and anorthosite genesis. Earth and Planetary Science Letters 38, 249–272.

Duchesne, J.C., Hertogen, J., 1988. Le magma parental du lopolithe de Bjerkreim-Sokndal (Norvège méridionale). Comptes rendus de l'Académie des sciences. Paris 306 (2), 45–48.

Duchesne, J.C., Maquil, R., 2001. The Egersund-Ogna massif. In: Duchesne, J.C. (Ed.), The Rogaland Intrusive Massifs—An Excursion Guide. Norges Geologisk Undersokelse, Trondheim, pp. 25–34.

Duchesne, J.C., Wilmart, E., 1997. Igneous charnockites and related rocks from the Bjerkreim-Sokndal layered intrusion (southwest Norway): a jotunite (hypersthene monzodiorite)-derived A-type granitoid suite. Journal of Petrology 38 (3), 337–369.

Duchesne, J.C., Roelandts, I., Demaiffe, D., Hertogen, J., Gijbels, R., De Winter, J., 1974. Rare-earth on monzonoritic rocks related to anorthosites and their bearing on the nature of the parental magma of the anorthositic series. Earth and Planetary Science Letters 24, 325–335.

Duchesne, J.C., Roelandts, I., Demaiffe, D., Weis, D., 1985. Petrogenesis of monzonoritic dykes in the Egersund-Ogna anorthosite (Rogaland, SW Norway): trace elements and isotopic (Sr, Pb) constraints. Contributions to Mineralogy and Petrology 90, 214–225.

Duchesne, J.C., Denoiseux, B., Hertogen, J., 1987a. The norite-mangerite relationships in the Bjerkreim-Sokndal layered lopolith (southwest Norway). Lithos 20, 1–17.

Duchesne, J.C., Demaiffe, D., Wilmart, E., 1987b. Fidsel-Värdefjell-Itland, Hidra massif and enveloppe. In: Maijer, C., Padget, P. (Eds.), The Geology of Southernmost Norway. Norges Geologiske Undersokelse Special Publication, pp. 42–47.

Duchesne, J.C., Ernst, G., Hertogen, J., 1991. Leuconoritic dykes: new evidence for injected crystal mushes from the Løyning lens (Egersund-Ogna massif, Rogaland, Norway) (abstract). IGCP 290, Adirondack Meeting, 13–19 Sept. 1991.

Emslie, R.F., 1980. Geology and petrology of the Harp Lake complex, central Labrador: an example of Elsonian magmatism. Geological Survey of Canada Bulletin 293 (136 pp.).

Emslie, R.F., 1985. Proterozoic anorthosite massifs. In: Tobi, A.C., Touret, J.L.R. (Eds.), The Deep Proterozoic Crust in the North Atlantic Provinces. Nato Advanced Study Institute, Reidel, Dordrecht, pp. 39–60.

Emslie, R.F., Hamilton, M.A., Thériault, R.J., 1994. Petrogenesis of a Mid-Proterozoic Anorthosite–Mangerite–Charnockite–Granite (AMCG) complex: isotopic and chemical evidence from the Nain Plutonic Suite. Journal of Geology 102, 539–558.

Ernst, G., 1990. La lentille de Löyning (Rogaland, Norvège méridionale). Master Thesis, Liège. 82 pp.

Ernst, G., Duchesne, J.C., 1991. Evidence of ultra-small layered intrusion: the Löyning lens, Egersund, Norway. Terra Abstracts 3, 426–427.

Fram, M., Longhi, J., 1992. Phase equilibria of dikes associated with Proterozoic anorthosites complexes. American Mineralogist 77, 605–616.

Fuhrman, M., Frost, B., Lindsley, D., 1988. Crystallization conditions of the Sybille monzosyenite, Laramie anorthosite complex, Wyoming. Journal of Petrology 29, 699–729.

Hibbard, M., Watters, R., 1985. Fracturing and diking in incompletely crystallized granitic plutons. Lithos 18, 1–12.

Holland, T., Babu, E., Walters, D., 1996. Phase relations of osumilite and dehydration melting in pelitic rocks: a simple thermodynamic model for the KFMASH system. Contributions to Mineralogy and Petrology 124, 423–439.

Jansen, B., Blok, A., Scheelings, M., 1985. Geothermometry and geobarometry in Rogaland and preliminary results from the Bamble area, south Norway. In: Tobi, A., Touret, J.L.R. (Eds.), The Deep Proterozoic Crust in the North Atlantic Provinces. Nato Advanced Study Institute, Reidel, Dordrecht, pp. 499–518.

Johnson, M., Anderson, A., Rutherford, M., 1994. Pre-eruptive volatile contents of magmas. In: Carroll, M., Holloway, J. (Eds.), Volatiles in Magmas. Mineralogical Society of America, pp. 281–330.

Jones, W., Peoples, J., Howland, A., 1960. Igneous and tectonic structures of the Stillwater complex, Montana. US Geologica Survey Bulletin 1071-H, 281–335.

Kolker, A., Lindsley, D.H., 1989. Geochemical evolution of the Maloin Ranch pluton, Laramie anorthosite complex, Wyoming: petrology and mixing relations. American Mineralogist 74, 307–324.

Krause, H., Pedall, K., 1980. Fe–Ti mineralizations in the Åna-Sira anorthosite, southern Norway. In: Siivola, J. (Ed.), Metallogeny of the Baltic Shield. Geological Survey of Finland, pp. 56–83.

Krause, H., Gierth, E., Schott, W., 1985. Fe–Ti deposits in the South Rogaland igneous complex, especially in the Anorthosite-massif of Åna-Sira. Norges Geologisk Undersokelse 402, 25–37.

Kress, V., Carmichael, I., 1991. The compressibility of silicate liquids containing Fe_2O_3 and the effect of composition, temperature, oxygen fugacity and pressure on their redox state. Contributions to Mineralogy and Petrology 108, 82–92.

Lange, R., 1994. The effect of H_2O, CO_2 and F on the density and viscosity of silicate melts. In: Carroll, M., Holloway, J. (Eds.), Volatile in Magmas. Mineralogical Society of America, pp. 331–369.

Lange, R., Carmichael, I., 1990. Thermodynamic properties of silicate liquids with emphasis on density, thermal expansion and

compressibility. In: Nicholls, J., Russell, J. (Eds.), Modern Methods of Igneous Petrology. Reviews in Mineralogy, pp. 25–64.
Longhi, J., 2005. A mantle or mafic crustal source for Proterozoic anorthosites? Lithos 83, 183–198.
Longhi, J., Fram, M., Vander Auwera, J., Montieth, J., 1993. Pressure effects, kinetics, and rheology of anorthositic and related magmas. American Mineralogist 78, 1016–1030.
Longhi, J., Vander Auwera, J., Fram, M., Duchesne, J.C., 1999. Some equilibrium constraints on the origin of Proterozoic (Massif) Anorthosites and related rocks. Journal of Petrology 40, 339–362.
Marker, M., Schiellerup, H., Meyer, G.B., Robins, B., Bolle, O., 2003. Geological map of the Rogaland Anorthosite Province (1:75000). In: Duchesne, J.C., Korneliussen, A. (Eds.), Ilmenite Deposits and their Geological Environments. Norges Geologiske Unsersøkelse, Trondheim.
Michot, P., 1960. La géologie de la catazone: le problème des anorthosites, la palingenèse basique et la tectonique catazonale dans le Rogaland méridional (Norvège méridionale). Norges Geologiske Unsersøkelse 212, 1–54.
Michot, J., 1961. The anorthositic complex of Haaland-Helleren. Norsk Geologisk Tidsskrift 41, 157–172.
Michot, P., 1965. Le magma plagioclasique. Geologische Rundschau 54, 956–976.
Michot, J., Michot, P., 1969. The problem of anorthosites. In: Isachsen, Y. (Ed.), Origin of Anorthosites and Related Rocks. N.Y. State Mus. Sci. Serv. Mem, pp. 399–410.
Morse, S.A., 1982. A partisan review of Proterozoic anorthosites. American Mineralogist 65, 1087–1100.
Morse, S., 1986. Convection in aid of adcumulus growth. Journal of Petrology 27, 1183–1214.
Möller, A., O'Brien, P., Kennedy, A., Kröner, A., 2002. Polyphase zircon in ultrahigh-temperature granulites (Rogaland, SW Norway): constraints for Pb diffusion in zircon. Journal of Metamorphic Geology 20, 727–740.
Möller, A., O'Brien, P., Kennedy, A., Kröner, A., 2003. Linking growth episodes of zircon and metamorphic textures to zircon chemistry: an example from the ultrahigh-temperature granulites of Rogaland (SW Norway). In: Vance, D., Villa, I., Müller, W. (Eds.), Geochronology: Linking the Isotope Record with Petrology and Textures. Special Publication. Geological Society of London, pp. 65–81.
Owens, B., Rockow, M., Dymek, R., 1993. Jotunites from the Grenville Province, Québec: petrological characteristics and implications for massif anorthosite petrogenesis. Lithos 30, 57–80.
Paludan, J., Hansen, U., Olesen, N., 1994. Structural evolution of the Precambrian Bjerkreim-Sokndal intrusion, south Norway. Norsk Geologisk Tidsskrift 74, 185–198.
Pasteels, P., Michot, J., 1975. Geochronologic investigation of the metamorphic terrain of southwestern Norway. Norsk Geologisk Tidsskrift 55, 111–134.
Philpotts, A.R., 1981. A model for the generation of massif-type anorthosites. Canadian Mineralogist 19, 233–253.
Rietmeijer, F., 1979. Pyroxenes from iron-rich igneous rocks in Rogaland, SW Norway. Geologica Ultrajectina 21 (341 pp.).
Robins, B., Tumyr, O., Tysseland, M., Garmann, L., 1997. The Bjerkreim-Sokndal layered intrusion, Rogaland, SW Norway: evidence from marginal rocks for a jotunite parent magma. Lithos 39, 121–133.
Schärer, U., Wilmart, E., Duchesne, J.C., 1996. The short duration and anorogenic character of anorthosite magmatism: U–Pb dating of the Rogaland complex, Norway. Earth and Planetary Science Letters 139, 335–350.
Scoates, J., 2000. The plagioclase-magma density paradox re-examined and the crystallization of Proterozoic anorthosites. Journal of Petrology 41 (5), 627–649.
Scoates, J.S., Frost, C.D., 1996. A strontium and neodymium isotopic investigation of the Laramie anorthosites, Wyoming, USA: implications for magma chamber processes and the evolution of magma conduits in Proterozoic anorthosites. Geochimica et Cosmochimica Acta 60 (1), 95–107.
Sun, S.S., McDonough, W.F., 1989. Chemical and isotopic systematics of oceanic basalts: implications for mantle composition and processes. In: Saunders, A.D., Norry, M.J. (Eds.), Magmatism in the Ocean Basins. Geological Society Special Publication. Blackwell Scientific Publications, pp. 313–345.
Tomkins, H., Williams, I., Ellis, D., 2005. In situ U–Pb dating of zircon formed from retrograde garnet breakdown during decompression in Rogaland, SW Norway. Journal of Metamorphic Geology 23, 201–215.
Toplis, M., Dingwell, D., Libourel, G., 1994. The effect of phosphorous on the iron redox ratio, viscosity, and density of an evolved ferrobasalt. Contributions to Mineralogy and Petrology 117, 293–304.
Vander Auwera, J., Duchesne, J.C., 1990. Evidence of Leuconoritic Liquids in the Egersund-Ogna Massif-Type Anorthosite (abstract), IGCP 290 on Origin of Anorthosites, Bujumbura, Burundi.
Vander Auwera, J., Duchesne, J.C., 1996. Petrology and geochemistry of the noritic Hogstad layered body (Rogaland, southwestern Norway): evidence for a jotunitic parent magma. In: Demaiffe, D. (Ed.), Petrology and Geochemistry of Magmatic Suites of Rocks in the Continental and Oceanic Crusts. ULB-MRAC, Bruxelles, pp. 111–127.
Vander Auwera, J., Longhi, J., 1994. Experimental study of a jotunite (hypersthene monzodiorite): constraints on the parent magma composition and crystallization conditions (P, T, fO2) of the Bjerkreim-Sokndal layered intrusion (Norway). Contributions to Mineralogy and Petrology 118, 60–78.
Vander Auwera, J., Longhi, J., Duchesne, J.C., 1998a. A liquid line of descent of the jotunite (hypersthene monzodiorite) suite. Journal of Petrology 39 (3), 439–468.
Vander Auwera, J., Bologne, G., Roelandts, I., Duchesne, J.C., 1998b. Inductively coupled plasma-mass spectrometry (ICP-MS) analysis of silicate rocks and minerals. Geologica Belgica 1, 49–53.
Vander Auwera, J., Bogaerts, M., Liégeois, J.-P., Demaiffe, D., Wilmart, E., Bolle, O., Duchesne, J.C., 2003. Derivation of the 1.0–0.9 Ga ferro-potassic A-type granitoids of southern Norway by extreme differentiation from basic magmas. Precambrian Research 124, 107–148.
Wager, L., Brown, G., 1968. Layered Igneous Rocks. Oliver and Boyd, Edinburgh. 588 pp.
Watson, E., Green, T., 1981. Apatite/liquid partition coefficients for the rare earth elements and strontium. Earth and Planetary Science Letters 56, 405–421.
Weis, D., Frey, F., 1991. Isotope geochemistry of Ninetyeast Ridge basalts: Sr, Nd, and Pb evidence for the involvement of the Kerguelen hot spot. In: Weissel, J., Peirce, J., Taylor, E., Alt, J., et al. (Eds.), Proceedings of the Ocean Drilling Program. Scientific Results, vol. 121. Ocean Drilling Program, College Station, TX, pp. 591–610.
Westphal, M., Schumacher, J., Boschert, S., 2003. High-temperature metamorphism and the role of magmatic heat sources at the Rogaland anorthosite complex in southwestern Norway. Journal of Petrology 44 (6), 1145–1162.

Wiebe, R.A., 1990. Dioritic rocks in the Nain complex, Labrador. Schweizerische Mineralogische und Petrographische Mitteilungen 70, 199–208.

Wielens, J., Andriessen, P., Boelrijk, N., Hebeda, E.H., Priem, H.N.A., Verdurmen, E.A.Th., Verschure, R.H., 1981. Isotope geochronology in the high-grade metamorphic Precambrian of southwestern Norway: new data and reinterpretations. Norges Geologiske Undersokelse Bulletin 359, 1–30.

Wilmart, E., 1982. Série supracrustale, granito-gneiss et charnockites de l'enveloppe métamorphique du massif anorthositique d'Ana-Sira (Rogaland, Norvège méridionale), Master Thesis, Liège, 121 pp.

Wilmart, E., Demaiffe, D., Duchesne, J.C., 1989. Geochemical constraints on the genesis of the Tellnes ilmenite deposit, southwest Norway. Economic Geology 84, 1047–1056.

Wilson, J., Overgaard, G., 2005. Relationships between the layered series and the overlying evolved rocks in the Bjerkreim-Sokndal intrusion, southern Norway. Lithos 83, 277–298.

Wilson, J., Robins, B., Nielsen, F., Duchesne, J.C., Vander Auwera, J., 1996. The Bjerkreim-Sokndal layered intrusion, southwest Norway. In: Cawthorn, R. (Ed.), Layered Intrusions. Elsevier, Amsterdam, pp. 231–256.